이학박사학위논문

Sources and fluxes of dissolved organic matter in the coastal ocean: Applications of carbon and radium isotope tracers

연안해역에서 탄소와 라듐 동위원소를 활용한 용존유기물의 기원과 플럭스 추적

2020년 2월

서울대학교 대학원
지구환경과학부

이 신 아

Sources and fluxes of dissolved organic matter in the coastal ocean: Applications of carbon and radium isotope tracers

연안해역에서 탄소와 라듐 동위원소를 활용한
용존유기물의 기원과 플럭스 추적

지도 교수 김 규 범

이 논문을 이학박사 학위논문으로 제출함
2020년 1월

서울대학교 대학원
지구환경과학부
이 신 아

이신아의 이학박사 학위논문을 인준함
2019년 12월

위 원 장 황 점 식 (인)

부위원장 김 규 범 (인)

위 원 허 영 숙 (인)

위 원 신 경 훈 (인)

위 원 김 태 훈 (인)

Abstract

Sources and fluxes of dissolved organic matter in the coastal ocean: Applications of carbon and radium isotope tracers

Shinah Lee
School of Earth and Environmental Sciences
The Graduate School
Seoul National University

Dissolved organic matter (DOM) in coastal waters plays a significant role in the ecosystem and the biogeochemical cycling of carbon and nutrients of the ocean. The behavior and cycling of DOM are heavily dependent on its origin and composition. Although it is important to study sources and fluxes of DOM in aquatic environments, DOM dynamics in coastal regions are still poorly understood due to its complexity. Thus, in this study, various DOM components, including dissolved organic carbon (DOC) and nitrogen (DON), δ^{13}C-DOC, and fluorescent dissolved organic matter (FDOM), were measured in different coastal environmental settings in order to determine the sources and fluxes of DOM.

First, coastal bay waters were collected in Masan Bay, Korea, which is surrounded

by heavily industrialized cities, in two sampling campaigns (Aug. 2011 and Aug. 2016). In 2011, excess DOC was observed for higher-salinity (16–21) waters, indicating that the excess source inputs were mainly from marine autochthonous production according to the δ^{13}C-DOC values of −23.7‰ to −20.6‰, the higher concentrations of protein-like FDOM, and the lower DOC/DON (C/N) ratios (8–15). By contrast, the high DOC waters observed in high-salinity waters in 2016 were characterized by low FDOM, more depleted δ^{13}C values of −28.8‰ to −21.1‰, and high C/N ratios (13–45), suggesting that the excess DOC source is from terrestrial C3 plants by direct land-seawater interactions. This study shows that using multiple DOM tracers including δ^{13}C-DOC, FDOM, and C/N ratios is a powerful method for determining the complex sources of DOM in the coastal ocean.

Second, estuarine water samples were collected in Nakdong-River Estuary, the estuary of the longest river in Korea. The sampling was conducted every hour for 24 h in each month from October 2014 to August 2015 at a fixed flatform at the downstream from a dam. The concentrations of DOC and humic-like FDOM showed significant negative correlations against salinity (r^2=0.42–0.98, $p < 0.0001$), indicating that the river-originated DOM components are the major source and behave conservatively in the estuarine mixing zone. The extrapolated δ^{13}C-DOC values (-27.5‰ to – 24.5‰) in freshwater confirm that both components are mainly of terrestrial origin. The slopes of humic-like FDOM against salinity were 60-80% higher in the summer and fall, due to higher terrestrial production of humic-like FDOM. The slopes of protein-like FDOM against salinity, however, were 70-80% higher in spring, due to higher biological production in river water. These results suggest that there are large seasonal changes in

riverine fluxes of humic and protein-like FDOM to the ocean.

Third, seawater samples were collected in three different bays (Gwangyang Bay, Suyoung Bay, and Ulsan Bay), Korea to determine the sources, biogeochemical alteration, and fluxes of DOM and nutrients (dissolved inorganic nitrogen, DIN; dissolved organic nitrogen, DON; dissolved inorganic phosphate, DIP). Radium isotopes (^{223}Ra, ^{224}Ra, and ^{226}Ra) were also measured in order to determine water ages and fluxes. The water residence times of these three bays were approximately 15, 1.9, and 1.5 days. Ulsan Bay showed clear two (terrestrial and marine) end-member mixing trends for DOC, DIN, and DIP owing to a short water residence time. Suyoung Bay showed two different trends: one slope showed the two end-member sources mixing for DOC, DIN, and DIP, while the other trend showed significant "excess" DOC under depleted nutrients. The excess DOC observed in Suyoung bays is determined to be marine in origin based on δ^{13}C-DOC values. Gwangyang Bay, which had the longest residence time, showed almost completely depleted DIN and DIP, but large "excess" DOC and DON. The concentrations of terrestrial humic-like FDOM were conservatively mixed in three bays. The net fluxes of DOC and nutrients estimated using Ra-based water residence times suggest that Gwangyang Bay is a significant source of DOC and DON but a sink of DIN and DIP, while Suyoung and Ulsan bays are the sources of inorganic nutrients. Thus, this study reveals that a residence time of coastal embayment plays an important role in biogeochemical production and alteration of nutrients and DOM. This study also shows that using a combination of multiple DOM tracers such as δ^{13}C-DOC, FDOM, and C/N ratios, together with Ra isotopes, is a powerful method for discriminating between the complex sources of DOM, and fluxes of DOM and nutrients in the coastal ocean.

Keyword: Dissolved organic carbon; Fluorescent dissolved organic matter; Dissolved organic nitrogen; Stable carbon isotope; Radium isotope; Coastal ocean

Student Number : 2010-23135

Table of Contents

List of tables

List of figures

1. Introduction

1.1. DOM in coastal ocean

Dissolved organic matter (DOM) plays an important role in biogeochemical cycles (e.g., de-oxygenation, acidification, photochemistry) and ecosystems of the ocean (Hansell and Carlson, 2002). DOM composition depends on its parent organic matter and subsequent biogeochemical processes. DOM in coastal waters originates from various sources including (1) *in situ* production by primary production, exudation of aquatic plants, and their degradation (Markager et al., 2011; Carlson and Hansell, 2015); (2) terrestrial sources by the degradation of soil and terrestrial plant matter (Opsahl and Benner, 1997; Bauer and Bianchi, 2011); and (3) anthropogenic sources (Griffith and Raymond, 2011).

Depending on the origin and composition of DOM, its behavior and cycling are different: a labile fraction of DOM is decomposed rapidly through microbially or photochemically mediated processes, whereas refractory DOM is resistant to degradation and can persist in the ocean for millennia. In the coastal ocean, organic matter from terrestrial plant litter or soils appears to be more refractory (Cauwet, 2002) and thus often behaves conservatively. In addition, refractory DOM is produced in the ocean by bacterial transformation of labile DOM by reshaping its composition (Tremblay and Benner, 2006; Jiao et al., 2010).

1.2. Source of DOM in coastal ocean

There are many approaches to distinguish the source of DOM in coastal areas using various tracers (Faganeli et al., 1988; Benner and Opsahl, 2001; Chen et al., 2004; Baker and Spencer, 2004; Cawley et al., 2012; Lee and Kim, 2018). The stable carbon isotopic composition of dissolved organic carbon (δ^{13}C-DOC) has been used to distinguish different sources. In general, δ^{13}C values derived from C3 and C4 land plants are in the range of −23‰ – −34‰ and −9‰ – −17‰ (Deines, 1980), respectively, while those derived from marine phytoplankton range from −18 to −22‰ (Kelley et al., 1998; Coffin and Cifuentes, 1999). Peterson et al. (1994) utilized δ^{13}C-DOC to distinguish the sources of DOC in four different bays. Similarly, Wang et al., (2004) determined δ^{13}C-DOC to determine the sources and transport of DOC in the Mississippi River estuary and adjacent coastal area.

Generally, DOC includes fluorescent dissolved organic matter (FDOM), which emits fluorescent light due to its chemical characteristics. As FDOM accounts for 20–70% of the DOC in coastal waters (Coble, 2007) and controls the penetration of harmful UV radiation in the euphotic zone, it plays a critical role in carbon cycles as well as biological production. FDOM have been successfully used for characterizing DOM (Coble et al., 1990; Coble, 1996). Fluorescence excitation-emission matrices and parallel factor analysis (EEM-PARAFAC) technique has been applied to trace the source of humic-like versus protein-like DOM in coastal waters and estuaries (Chen et al., 2004; Jaffé et al., 2004; Murphy et al., 2008).

DOC/DON ratios are often used to differentiate allochthonous versus

autochthonous sources. The C/N ratios of terrestrial organic carbon are usually higher than 12, while those of marine organic carbon from phytoplankton are almost constant ranging from 6 to 8 (Milliman et al., 1984; Lobbes et al.,2000).

However, the interpretation of isotopic ratio of bulk sample alone in complex coastal environments is somewhat complicated by the overlap of the isotopic ranges. Thus, several studies have used δ^{13}C-DOC combined with FDOM (Osburn and Stedmon, 2011; Osburn et al., 2011; Ya et al., 2015; Lu et al., 2015) or carbon isotope ratios combined with C/N ratio (Thornton and McManus, 1994; Andrews et al., 1998; Wang et al., 2004; McCallister et al., 2006; Pradhan et al., 2014) to discriminate different sources of DOM in estuarine and coastal waters. Because the interpretation of isotopic values is limited owing to the overlap of the isotopic value ranges, δ^{13}C-DOC values have been used often together with other tracers to better define different sources in the coastal ocean (Barros et al. 2010; Raymond and Bauer 2001b).

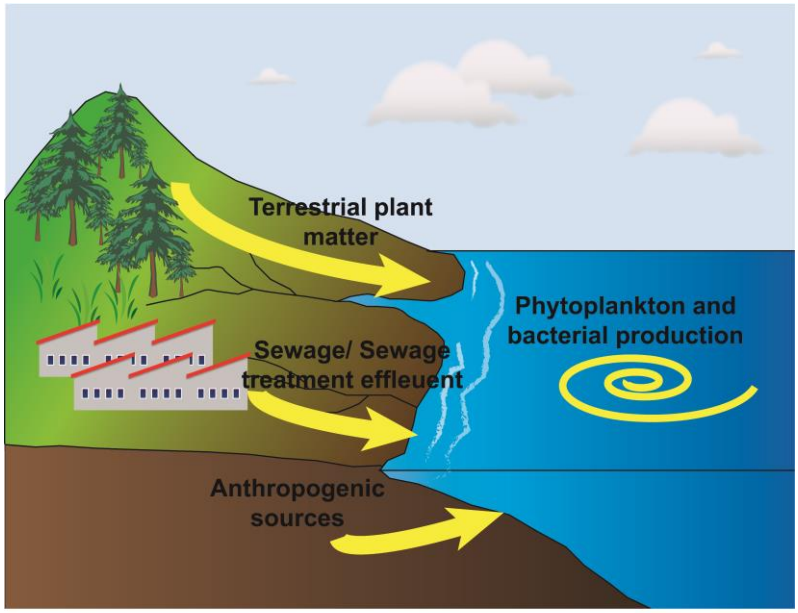

Figure 1.1. Source of DOM in coastal area.

1.3. Flux of DOM in coastal ocean

The flux of DOC in the ocean plays an important role in the global C budget (Bauer et al. 2013; Benner 2004; Hedges 1992). In general, terrestrial DOC is transported by river and surrounding watershed to the coastal ocean (Meybeck 1982; Spitzy and Ittekkot 1991). The global annual flux of DOC via rivers is approximately 0.17–0.36 × 10^{15} g (Meybeck, 1982; Ludwig et al., 1996; Dai et al., 2012). The DOC delivered from riverine discharges as well as *in situ* production through biological activities significantly affects carbon and biogeochemical cycles in coastal waters (Hedges, 1992; Bianchi et al., 2004; Bauer et al., 2013; Moyer et al., 2015).

The magnitudes of DOC and FDOM fluxes from rivers are generally dependent on rainfall, discharge, and temperature (Maie et al., 2006; Jaffé et al., 2004; Huang and Chen, 2009). In the estuarine mixing zone, intensive biogeochemical processes occur through photo-oxidation, microbial degradation, or physicochemical transformations (i.e., flocculation, sedimentation) (Bauer and Bianchi, 2011; Moran et al., 1991; Benner and Opsahl, 2001; Raymond and Bauer, 2001). Recent studies have demonstrated large seasonal variations as high as 40%, in DOC export from rivers to the ocean (Burns et al., 2008; Bianchi et al., 2004; Dai et al., 2012).

Although riverine fluxes of DOC and nutrients have been studied over the last a few decades (Williams, 1968; Schlesinger and Melack, 1981; ref), the other pathways of DOC and nutrients fluxes, including seawater-land interaction, submarine groundwater discharge, and atmospheric deposition. Bianchi et al., (2009) proposed that the inputs of photochemically-altered DOC from bay may provide an additional organic carbon source

for microbial food webs in the open ocean (northern Gulf of Mexico). Thus, it is important to evaluate the various inputs of terrestrial sources of DOC and nutrients in coastal waters and subsequent fluxes of biogeochemically transformed DOC and nutrients from coastal to the remote ocean.

1.4. Aim of this study

The objectives of this study are:

(1) To determine the behaviors of DOM in various regions including Masan Bay, Nakdong-River Estuary, Gwangyang Bay, Suyoung Bay, and Ulsan Bay in Korea

(2) To trace major sources of DOM in various region using multiple tracers including δ^{13}C-DOC, FDOM, and DOC/DON ratios.

(3) To calculate the fluxes of DOM from Nakdong-River estuary based on the slopes between salinities and DOM components.

(4) To estimate the fluxes of DOC in three different bays (Gwangyang Bay, Suyoung Bay, and Ulsan Bay) based on Radium-based water residence time.

2. Materials and Methods

2.1 Water sampling and storage

All water samples were filtered through pre-combusted GF/F filters. The FDOM samples were stored in pre-combusted amber glass vials and kept below 4°C in a refrigerator before analysis. The DOC, Total dissolved nitrogen (TDN), and δ^{13}C-DOC samples were acidified to pH ~2 using 6 M HCl to avoid bacterial activities and stored in pre-combusted glass ampoules. Ampoules were fire-sealed to prevent the samples from any contaminations. Samples analyzed for dissolved inorganic nitrogen (DIN), dissolved inorganic phosphate (DIP), and dissolved organic nitrogen (DON) were stored frozen in a HDPE bottle (Nalgene) or conical tube prior to analysis.

For ^{223}Ra and ^{224}Ra measurements, about 100L seawater was passed through an acrylic column which filled with 16 g (dry) of MnO_2-impregnated acrylic fiber (4.5 cm in diameter, 20 cm in length) with a flow rate of 1.0 L min^{-1} (Kim et al. 2001; Moore and Reid 1973).

2.2 Measurements of temperature and salinity

Salinity and temperature were measured using a YSI Pro Series conductivity probe sensor at the field stations right after sampling or in the laboratory. Salinity and temperature in Gwangyang Bay were measured by CTD (SBE 911+).

2.3 Analysis of DOC and DON

The concentrations of DOC and TDN were determined using a high-temperature catalytic oxidation (HTCO) analyzer (TOC-V_{CPH}, Shimadzu, Japan) (Fig. 2.1). The standardization for DOC analysis was performed using a calibration curve of acetanilide (C:N ratio = 8) in ultra-pure water. The acidified samples were purged with carbon dioxide (CO_2) free carrier gas for 2 min to remove inorganic carbon. The samples were then injected into a combustion column packed with Pt-coated alumina beads and heated to 720°C. The CO_2 evolving from combusted organic carbon was detected by a non-dispersive infrared detector (NDIR). Our DOC and TDN methods were verified using seawater reference samples for DOC of 44–46 μ mol L^{-1} and for TDN of 32–34 μ mol L^{-1}, which were produced by the University of Miami (Hansell's lab) in the USA. Inorganic nutrients were measured using nutrient auto-analyzers (Alliance Instruments, FUTURA+ for 2011 samples and QuAAtro39, SEAL Analytical Ltd. for 2016 samples). Reference seawater materials (KANSO Technos, Japan) were used for the verification of analytical accuracy. DON concentrations were calculated based on the difference between the TDN and DIN concentrations.

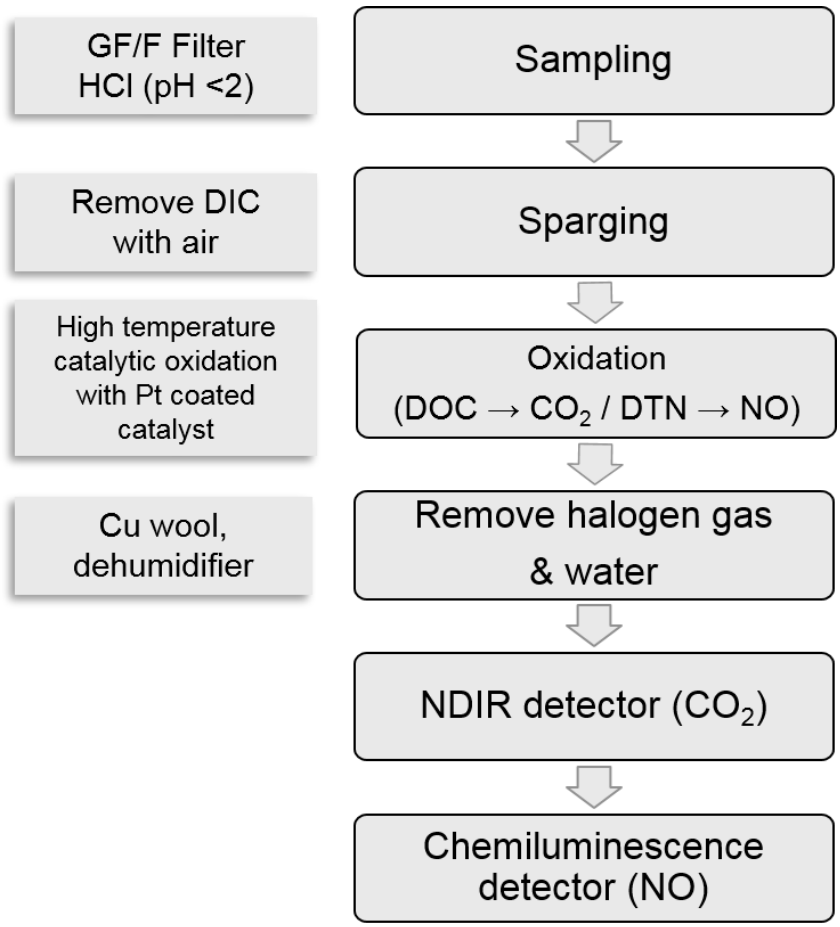

Figure 2.1. Schematic diagram of overall analytical procedures for the measurement of DOC concentration and TDN concentration using TOC analyzer (TOC-VCPH, Shimadzu, Japan).

2.4 Analysis of FDOM

FDOM was determined using a spectrofluorometer (FluoroMate FS-2, SCINCO) within two days from the sampling time (fig. 2.2). EEMs were collected for the emission (Em) wavelength range of 240–600 nm with 2 nm intervals and an excitation (Ex) wavelength range of 240–500 nm with 5 nm intervals. Each sample value was subtracted for the signal of Milli-Q water produced daily to remove Raman scattering peaks. All data were converted to ppb quinine sulfate equivalent (QSE) using a quinine sulfate standard solution dissolved in 0.1N sulfuric acid at Ex/Em of 350/450 nm. We did not correct EEM data for inner filter effects before measurements, because the inner filter effects were found to be negligible for coastal water samples using this instrument (Lee and Kim, 2018). FDOM was also determined by using a different spectrofluorometer (Horiba Aqualog). The scanning wavelength for EEMs was 250–600 nm with 3 nm increments for excitation and 210–600 nm with 2 nm increments for emission. All data were converted to the Raman unit (R.U.). The inner-filer effect was automatically corrected by this instrument.

Parallel factor analysis (PARAFAC) modeling was performed for each data set by MATLAB R2013a software (MathWorks INC., Natick, MA, USA) using the DOMFluor toolbox (Stedmon and Bro, 2008).

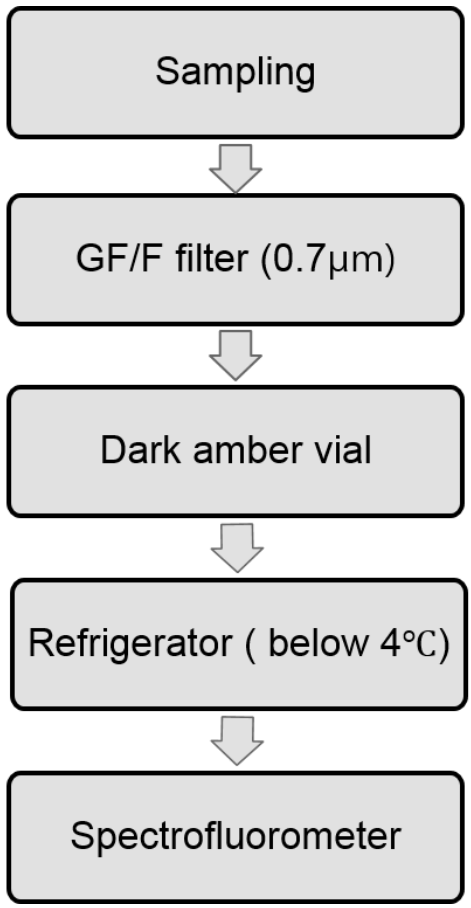

Figure 2.2. Schematic diagram of overall analytical procedures for the measurement of FDOM concentration.

2.5 Analysis of δ^{13}C-DOC

The values of δ^{13}C-DOC were measured using a TOC-IRMS instrument consisting of an IRMS instrument coupled with a Vario TOC cube (Isoprime, Elementar, Germany) (Figs. 2.4 and 2.5). The TOC instrument uses a common high-temperature catalytic combustion method (Kirkels et al., 2014) (Fig. 2.6). The analytical method is fully described in Kim et al. (2015). Briefly, 10 mL of filtered samples were purged with O_2 gas for 20–30 min to completely remove DIC after the samples were acidified to pH ~2. Then, 1 mL of the sample was injected into Pt-impregnated catalyst in a quartz tube. In this tube, the DOC was converted completely to CO_2 at 750°C, which was then fed through a water trap followed by a halogen trap. After DOC was detected by a NDIR detector, the CO_2 gas was entered the TOC-IRMS interface by the O_2 carrier gas. In the interface, the CO_2 was transferred to the IRMS instrument following the removal of any interfering gases (Fig. 2.7). The δ^{13}C-DOC value of blank was measured using the Low Carbon Water (LCW) from Hansell lab (University of Miami), which contains less than 2 μM DOC. Certified IAEA-CH6 sucrose (International Atomic Energy Agency, −10.45 ± 0.03‰) prepared with the low carbon water was used as a standard solution. A standard sample was analyzed for every sample queue (once before or after ten samples) to check a drifting effect during the measurements. The blank correction was performed using a method previously described in De Troyer et al. (2010) and Panetta et al. (2008). Our measurement result of δ^{13}C-DOC for the DSR (University of Miami) was −21.5 ± 0.1‰, which is consistent with the results reported by Panetta et al. (2008) and Lang et al. (2007). The reproducibility of TOC-IRMS was ~0.3‰.

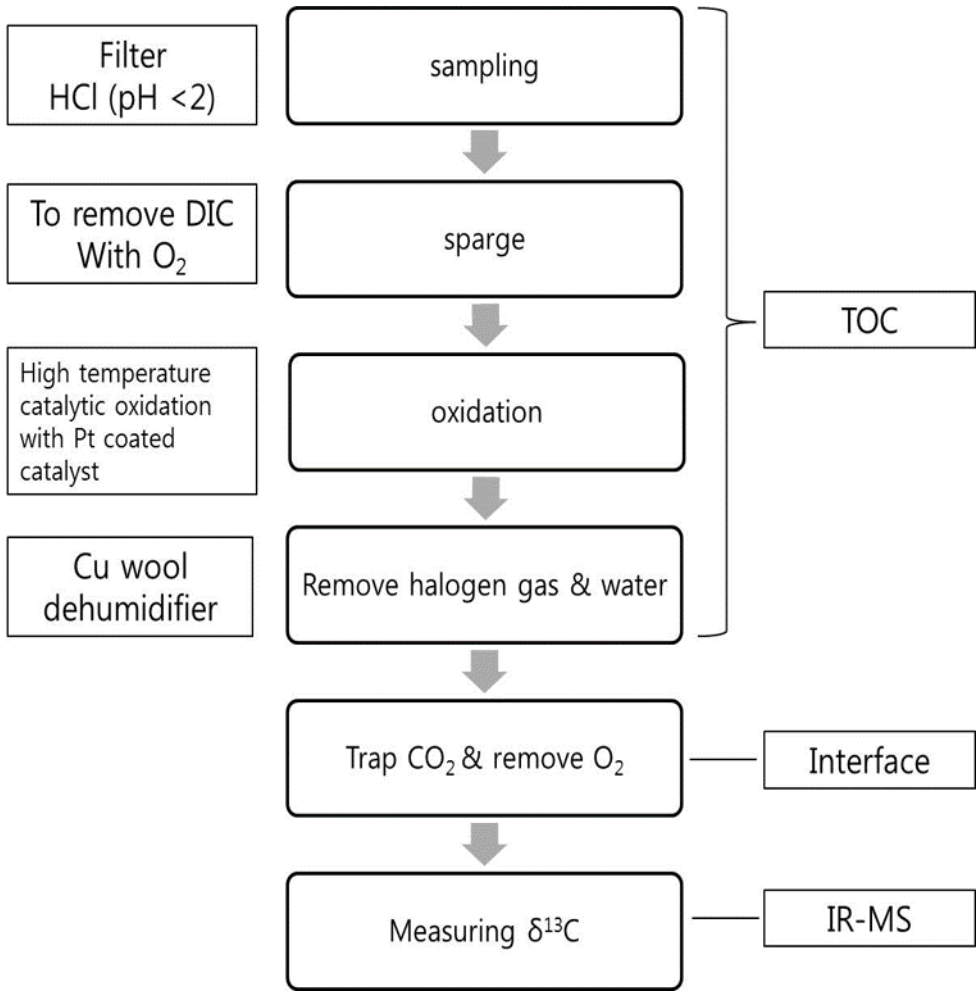

Figure 2.3. Schematic diagram of overall analytical procedures for the measurement of δ^{13}C-DOC signature.

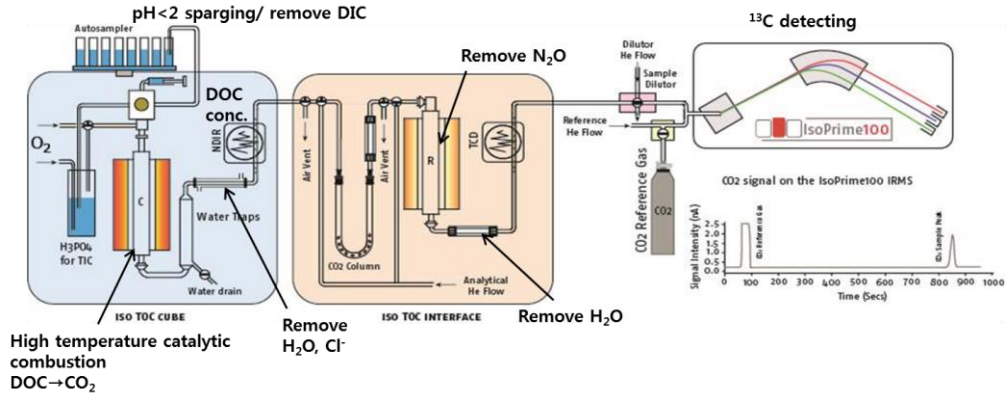

Figure 2.4. Schematic diagram of TOC-IRMS for measurement of δ^{13}C-DOC (from Isoprime manual).

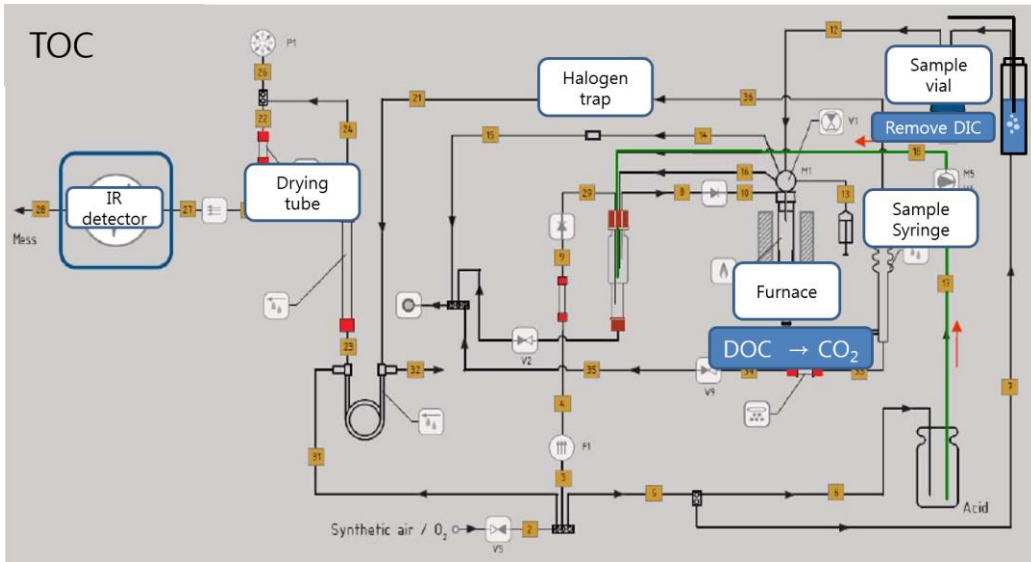

Figure 2.5. Schematic diagram of TOC analyzer for the measurement of δ^{13}C-DOC signature (modified From Elememtar VarioTOC cube manual).

2.6 Analysis of nutrients

Inorganic nutrients (DIN and DIP) were measured using nutrient auto-analyzers (QuAAtro39, SEAL Analytical Ltd). Verification of analytical accuracy was performed using reference seawater materials (KANSO Technos, Japan). We define DIN as the sum of NO_3^-, NO_2^-, and NH_4^+). Total dissolved nitrogen (TDN) was also measured using nutrient auto-analyzers after persulfate oxidation (Grasshof et al., 1999; Kwon et al., 2019). Deep seawater reference material (University of Miami, USA) was used to verify the accuracy. The concentrations of DON were calculated using the differences between DTN and DIN concentrations.

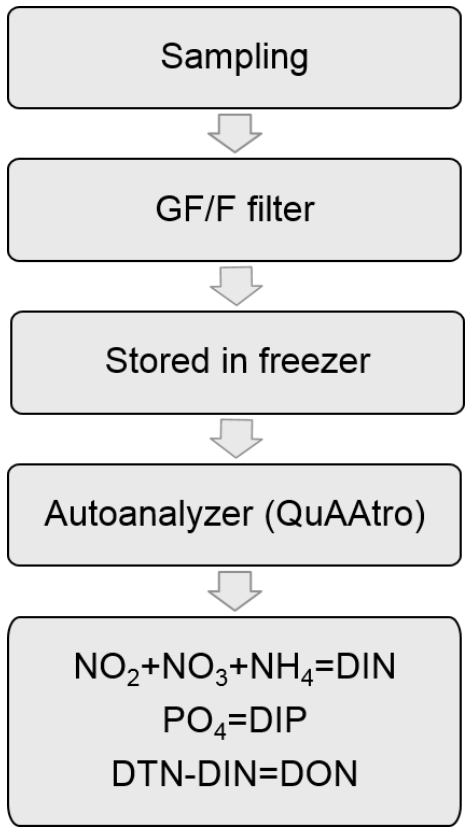

Figure 2.6. Schematic diagram of nutrient auto-analyzer for the measurement of nutrients (QuAAtro39, SEAL Analytical Ltd).

2.7 Analysis of Ra isotopes

For ^{223}Ra and ^{224}Ra activities, the collected samples were rinsed with deionized water to wash off any sea salts and properly adjusted the moisture content to 1:1 ratio of water and fiber (Sun and Torgersen, 1998). The ^{223}Ra and ^{224}Ra activities were determined using a delayed coincidence counter (RaDeCC) (Moore and Arnold, 1996). The sample efficiency was corrected using a MnO_2-fiber with ^{227}Ac and ^{232}Th standard. After the measurements of ^{223}Ra and ^{224}Ra activities, a MnO2-fiber were ashed in a furnace at 820°C and stored in gamma vials (Kim et al., 2003). The ^{226}Ra activities were determined using a well-type gamma-ray spectrometer.

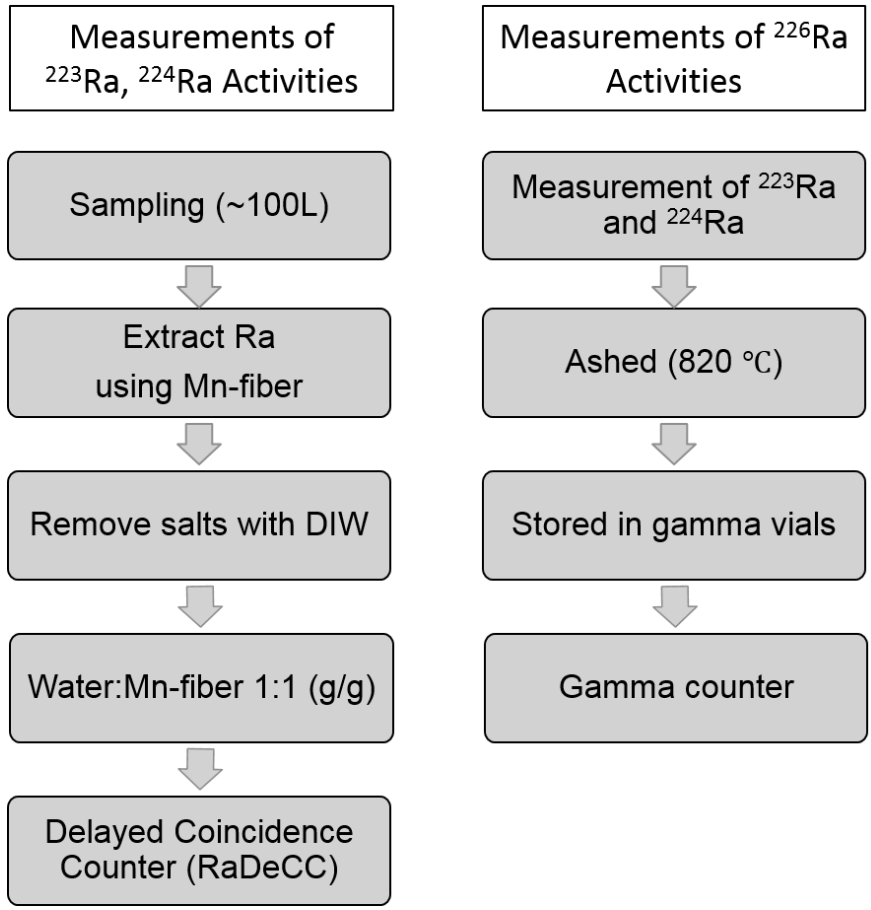

Figure 2.7. Schematic diagram of the analytical procedure for the measurement of ^{223}Ra, ^{224}Ra, and ^{226}Ra in seawater.

3. Tracing terrestrial versus marine sources of dissolved organic carbon in a coastal bay using stable carbon isotopes

3.1 Introduction

Masan bay is surrounded by cities with thousands of industrial plants and a population of 1.1 million. In association with large anthropogenic nutrient loading, this area has been recognized as a highly eutrophic embayment (Lee and Min, 1990; Yoo, 1991; Hong et al., 2010). Red tides and hypoxic water mass in the bottom layer of the bay have occurred annually in spring and summer (Lee et al., 2009). In addition, there are potential point sources of sewage treatment plants (STPs) which manage domestic and industrial wastewater from Masan and Changwon cities. Lee et al. (2011) revealed the origins of sewage and organic matter using dissolved sterols in Masan Bay. They reported that the water samples from the creeks, inner bay, and nearby STP were affected by sewage sources. Oh et al. (2017) showed that the excess DOC in bay water is produced by phytoplankton production. Therefore, Masan Bay is a suitable place to test the applicability of these multiple tracers to differentiate complicated DOM sources in other areas of the world's coastal regions.

3.2 Study area and sampling

3.2.1 Study area

Masan Bay is located on the southeast coast of Korea with an area of approximately 80 km^2 (Fig. 3.1). The annual precipitation is approximately 1500 mm, and most of the precipitations occurs in the summer monsoon season. The amount of freshwater discharge into this bay is approximately 2.5×10^8 m^3 yr^{-1} with significant seasonal variation. The tide is semi-diurnal, showing a maximum tidal amplitude of ~1.9 m (average = 1.3 m) during the sampling period. Due to topographic conditions, the current is very weak (2–3 cm s^{-1}), and the residence times of water in the inner bay and in the entire bay are approximately 54 and 23 days, respectively (Lee et al., 2009). In the middle of the bay, an artificial island was constructed in 2015–2016 (Fig. 3.1) with an area of 0.64 km^2. There is no marsh or wetland habitat. The artificial island may have resulted in changes in water currents, residence times, and biogeochemical conditions.

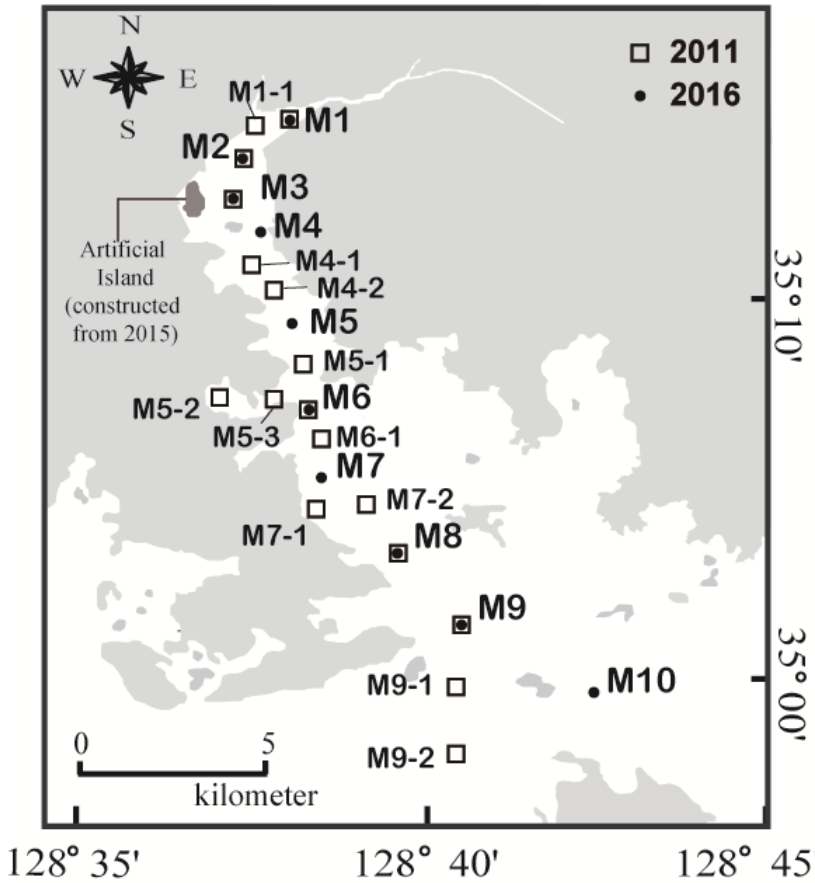

Figure 3.1. A map showing the sampling stations for DOC, δ^{13}C-DOC, FDOM, and DOC/DON ratio in Masan Bay, Korea, in 2011 and 2016.

3.2.2 Sampling

Sampling was conducted in August 2011 and August 2016 in Masan Bay. Water samples were collected from the surface at 17 sites in 2011 and 10 sites in 2016, from the inner to the outer bay. The bay receives a large amount of freshwater discharge from the northernmost part of the region. The averages of surface water temperature were 30.4 ± 2.3°C in 2011 and 26.5 ± 0.7°C in 2016.

3.3 Results and discussion

3.3.1 Horizontal distributions of DOM

The salinity of surface seawater in August 2011 ranged from 10 to 21, while the salinity in August 2016 ranged from 25 to 32 (Table 3.1). The concentrations of DOC in both sampling periods ranged from 100 μM to 200 μM (Table 3.1), which fall within the DOC ranges commonly observed in coastal waters (Gao et al., 2010; Osburn and Stedmon, 2011; Kim et al., 2012). The highest concentration of DOC in 2011 (186 μM) was observed at station M4-1 in the middle of the bay, whereas the highest concentration of DOC in 2016 (191 μM) was observed at station M1, which is the innermost station in the bay (Fig. 3.2). DOC concentrations were lowest at the outermost stations in both sampling periods. Concentrations of DON were in the range of 7–24 μM in 2011 and 3–15 μM in 2016, with the highest value at M5-1 in 2011 and at M1 in 2016 (Table 3.1).

EEM-PARAFAC dataset analyses identified three components in the surface water samples. EEMs contour plots and split-half validation results of three components are shown in Fig. 3.3 and 3.4. Based on the comparison with the data in the OpenFluor (Murphy et al., 2014), Component 1 ($FDOM_H$, Ex/Em = 322/405 nm) is associated with a terrestrial humic-like component (Liu et al., 2019; Dalmagro et al., 2019; Chen et al., 2016). Component 2 ($FDOM_M$, Ex/Em = 386/450 nm) is also associated with an allochthonous humic-like component (Wünsch et al., 2017). Component 3 ($FDOM_P$,

Ex/Em = 280/330 nm) is associated with a protein-like component, which is a product of microbial processes (Liu et al., 2019; Murphy et al., 2011; Osburn et al., 2011). We use Component 1 as a representative of terrestrial humic-like FDOM ($FDOM_H$) in this study because there was a good correlation (r^2 =0.95) between Component 1 and Component 2.

$FDOM_H$ is known to indicate humic substances from terrestrial, anthropogenic, or agricultural sources (Coble, 2007), whereas $FDOM_P$ is likely related to autochthonous or anthropogenic sources (Coble, 1996; Hudson et al., 2007). The intensities of $FDOM_H$ and $FDOM_P$ in 2011 were in the range of 3.6–9.2 ppb QSE and 4–79 ppb QSE, respectively (Fig. 3.5). The intensities of $FDOM_H$ and $FDOM_P$ in 2016 were in the range of 2.7–0.6 ppb QSE and 4.8–2.1 ppb QSE, respectively (Fig. 3.5). An exceptionally higher concentration of $FDOM_P$ was observed at station M4-1 (78 ppb QSE) relative to that of other stations (2–25 ppb QSE) in 2011 (Fig. 3.5).

Table 3.1. Salinity, DOC, $FDOM_H$, $FDOM_P$, and δ^{13}C-DOC in surface water of Masan Bay in August 2011 and August 2016.

sampling campaign	station	salinity	DOC	$FDOM_H$	$FDOM_T$	δ^{13}C-DOC	DON	DOC/DON
			μM	ppbQSE	ppbQSE	‰	μM	
Aug. 2011	M1	14.0	148	6.7	13.6	−25.4	12	12
	M1-1	12.8	151	9.2	14.3	−24.3	7	21
	M2	10.2	157	9.0	5.4	−24.6	11	14
	M3	16.3	147	8.2	14.7	n/a	16	9
	M4-1	19.0	186	7.1	78.7	−21.9	13	15
	M4-2	18.6	155	6.9	8.3	−21.6	10	15
	M5-1	17.7	138	4.5	4.5	−23.3	24	6
	M5-2	18.4	133	5.8	20.9	−24.5	11	12
	M5-3	18.9	135	8.0	11.3	−23.7	13	11
	M6	18.4	146	6.6	24.8	−23.3	19	8
	M6-1	19.2	142	5.5	7.4	n/a	9	15
	M7-1	19.5	157	5.8	10.5	−20.6	11	15
	M7-2	18.9	148	5.6	9.6	−21.5	12	12
	M8	19.5	152	5.6	7.6	−21.5	15	10
	M9	18.8	149	5.6	14.5	−21.9	10	15
	M9-1	19.1	154	5.1	10.2	−21.0	12	13
	M9-2	20.8	106	3.6	13.1	−22.0	8	13
Aug. 2016	M1	29.2	191	2.7	4.8	−22.8	15	13
	M2	29.9	164	2.0	3.4	−21.1	7	22
	M3	26.0	155	2.5	3.8	−28.8	8	19
	M4	27.4	149	1.9	3.5	−22.6	9	17
	M5	25.5	165	1.8	3.3	−23.5	10	16
	M6	30.5	147	1.1	3.0	−23.7	6	26
	M7	31.4	166	1.3	4.4	−26.2	4	45
	M8	32.0	123	0.8	2.3	−23.7	5	26
	M9	32.0	146	0.6	2.1	−24.4	5	30
	M10	31.9	130	0.7	2.7	−25.0	3	39

n/a = not available.

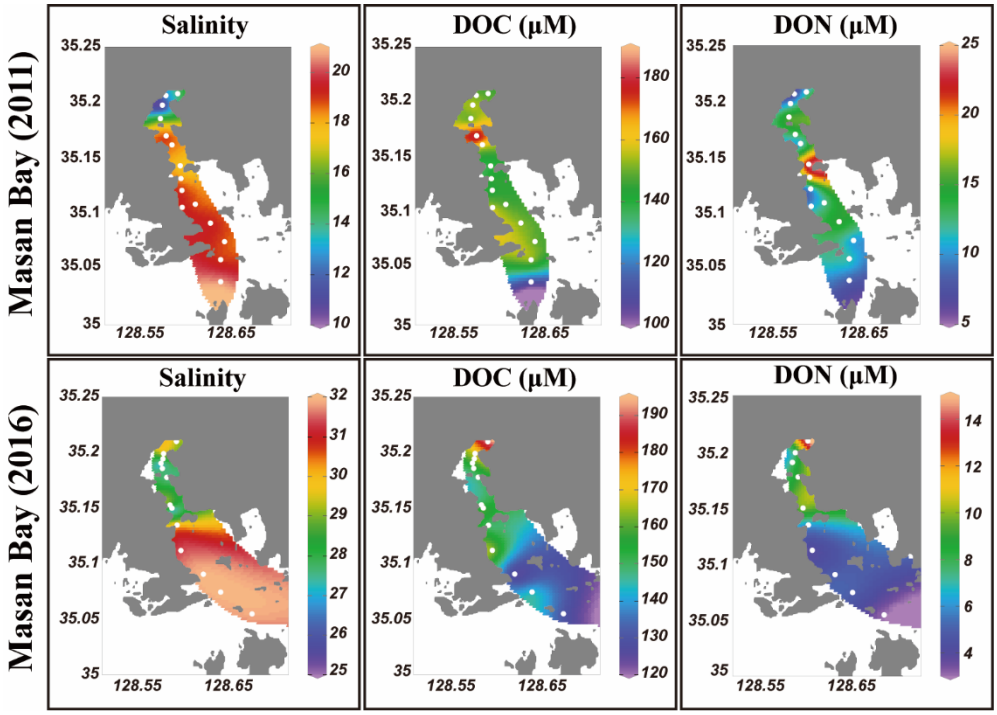

Figure 3.2. Surface distributions of salinity, DOC, and DON in Masan Bay, Korea, in 2011 and 2016.

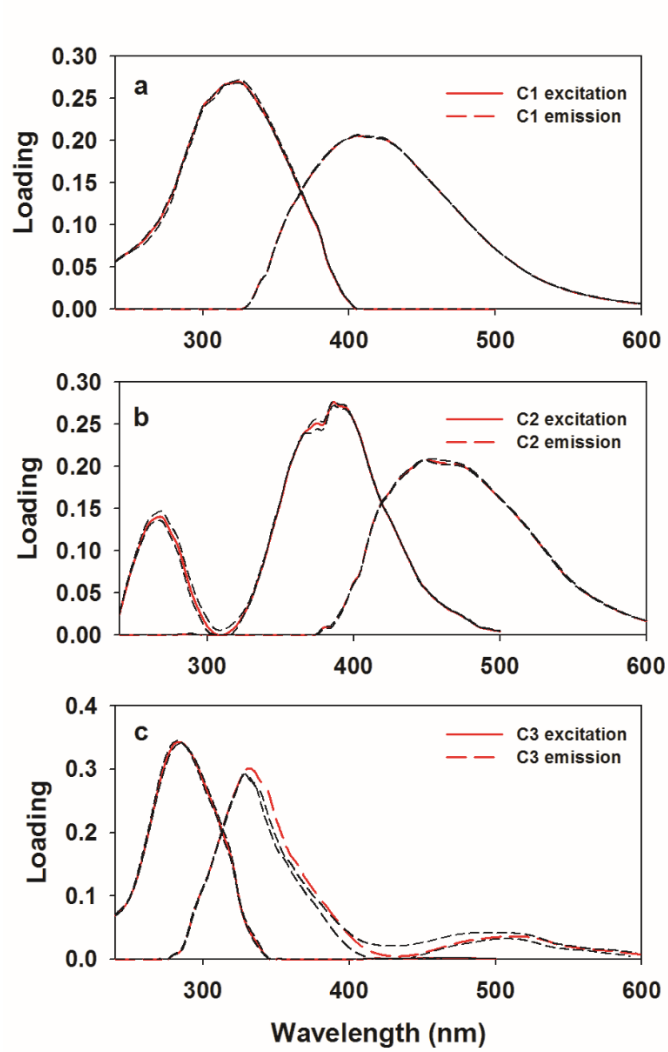

Figure 3.3. Split-half validation results for three components identified in the Masan Bay. a) component 1, b) component 2, and c) component 3. Excitation (red solid line) and emission (red dashed line) and the split (black short dashed lines) spectra are shown.

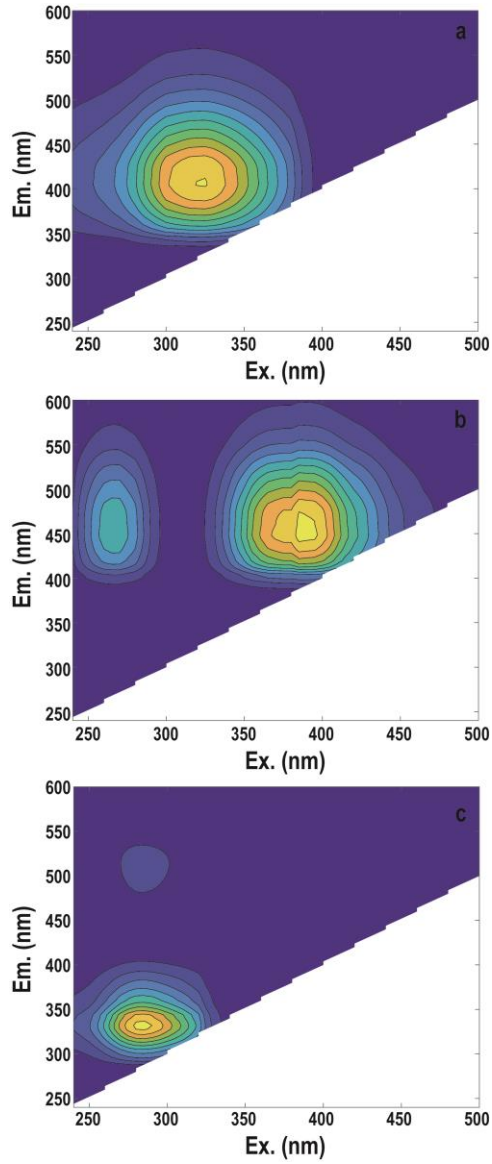

Figure 3.4. EEM contour plots of the three PARAFAC component in Masan Bay. a) component 1 ($FDOM_M$, Ex = 290–320 nm, Em = 370–420 nm), b) component 2 ($FDOM_H$, Ex = 320–360 nm, Em = 420–460 nm), and c) component 3 ($FDOM_P$, Ex = 275–300 nm, Em = 340–360 nm).

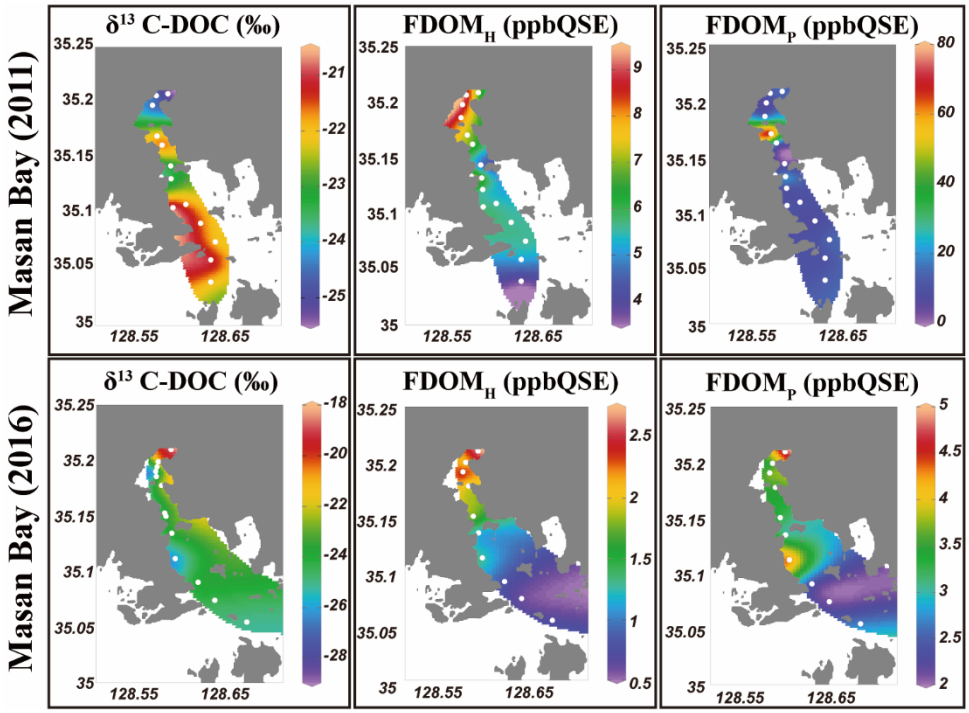

Figure 3.5. Surface distributions of δ^{13}C-DOC, $FDOM_H$, and $FDOM_P$ in Masan Bay, Korea, in 2011 and 2016.

3.3.2 Origin of excess DOM

The plot of DOC against salinity in 2011 showed two different mixing trends. The first slope showed a slight increase in DOC with decreasing salinity toward the innermost stations, including M1, M1-1, and M2 (Fig.3.6a, Group 1). The second trend showed a sharp rise in DOC (excess DOC in 2011) to the maximum at stations with salinities between 18 and 22 (Fig.3.6a, Group 2), indicating that there are other DOC sources at the high-salinity stations, besides the two end-member mixing. The plot of DOC against salinity showed that DOC in 2016 was in a range similar to that of 2011, although there was much less influence from fresh water (Fig. 3.6a, Group 3). This plot shows that there was an addition of DOC (excess DOC) in 2016 for high-salinity water in the bay. The potential sources of excess DOC occurring in this bay water may include terrestrial freshwater in creeks, STP water, direct land-seawater interaction, and in-situ biological production. The creek water may include various anthropogenic sources (i.e., industrial, agricultural, and domestic sewage) as well as natural land sources. There are no salt-marsh or wetland habitat in Masan Bay. To determine the main sources of the excess DOC using δ^{13}C-DOC, FDOM, and DOC/DON ratios, the excess DOC stations are separated into three groups (Fig. 3.6a).

Group 1 includes low-salinity water stations (M1, M1-1, M2, M3, M5-1, M5-2, and M5-3) observed in 2011. δ^{13}C-DOC values for Group 1 ranged from −25.4‰ to −23.3‰. We plotted a conservative mixing curve of δ^{13}C-DOC for two end-member mixing (Spiker, 1980; Raymond and Bauer, 2001). The assumed end-member values of

DOC and δ^{13}C-DOC were 185 μM and −28‰, respectively, for the terrestrial end-member (S=0) and 100 μM and −18‰, respectively, for the marine end-member (S=34). The δ^{13}C values of Group 1 fall into the mixing line or were slightly heavier than the mixing line within 1.5 ‰, indicating the conservative mixing between the terrestrial C3 land plant (−23‰ to −32‰) in freshwater and the open ocean seawater. The slightly heavier values could be produced by in-situ biological mixing during the mixing processes. As such, the plot of δ^{13}C-DOC values versus C/N ratios also indicates that the excess DOC of Group 1 is from freshwater DOC (Fig. 3.7).

Group 2 includes high-salinity water stations (M4-1, M4-2, M6, M6-1, M7-1, M7-2, M8, M9, and M9-1) observed in 2011. The δ^{13}C-DOC values of Group 2 were in the range of −23.3‰ to −20.6‰ and were more enriched than the conservative mixing curve. These values are close to the marine δ^{13}C-DOC values (−22 to −18‰) (Fry et al., 1998), except for one station (M6), in this group (−23.3‰). The δ^{13}C-DOC values of Group 2 suggest that DOM was added *in situ* by biological production in seawater. As such, the plot of δ^{13}C-DOC values versus C/N ratios also indicates that the excess DOC of Group 2 is produced by marine phytoplankton (Fig. 3.7).

Group 3 includes high-salinity water stations (M1, M2, M3, M4, M5, M6, and M7) observed in 2016. Although all data were collected in the same wet season (August), the salinity ranges of both campaigns were different from those in 2011, with a narrow high salinity range in 2016. The δ^{13}C-DOC values for Group 3 also showed significantly different values relative to those sampled in 2011 (Group 1 and Group 2). The δ^{13}C-DOC

values for Group 3 were depleted (−28.8‰ and −21.1‰) relative to the conservative mixing curve (Fig. 3.6b). The plot of δ^{13}C-DOC values versus C/N ratios indicates that the excess DOC of Group 3 is from C3 terrestrial plants through direct land-seawater interactions based on the fact that the excess DOC occurred in high-salinity (26–32) waters (Fig. 3.7).

$FDOM_H$ showed a significant negative correlation with salinity ($r^2 = 0.89$). The concentrations were highest for Group 1 and lowest for Group 3. This result indicates that humic DOM in this region was mainly from a terrestrial source and behaved conservatively in the freshwater and seawater mixing zone. This trend is commonly observed in coastal waters worldwide (Coble et al., 1998; Mayer et al., 1999). However, the concentration of $FDOM_P$ showed no correlation with salinity. In general, $FDOM_P$ shows non-conservative behavior in many estuaries owing to the extra source of DOC produced by *in situ* biological production (Benner and Opsahl, 2001). In the study region, a remarkably high $FDOM_P$ concentration was observed at station M4-1 in 2011, where DOC concentration was highest. This trend also supports the argument based on the δ^{13}C-DOC results, where the main source of DOC at this station is from *in situ* biological production (Twardowski and Donaghay, 2001; Zhang et al., 2009). Except M4-1 station, we observed the decoupling between DOC and $FDOM_H$ because $FDOM_H$ is not the major portion of DOC in this bay.

Masan Bay has many potential land sources of DOM from different creeks. In addition, the treated sewage outflow from a STP is located near station M7-1 (Fig. 3.1).

Many studies have been conducted to identify organic pollutants from STP (Kannan et al., 2010; Lee et al., 2011). In our study, however, station M7-1 did not show different DOM characteristics: (1) the concentrations of DOC, $FDOM_H$, and $FDOM_P$ against salinity did not show anomalously higher or lower trends, relative to the other stations nearby. (2) The δ^{13}C-DOC values at M7-1 (−20.6‰) were close to the marine values, similar to those in other stations nearby, although they are known to be lighter in some US wastewater treatment plants (−26‰) (Griffith et al., 2009). (3) A fulvic-like peak was not observed, although a significantly higher fulvic-like peak (Ex/Em 320–340 nm/410–430 nm) was observed in treated sewage (Baker and Inverarity, 2004). (4) The increase of $FDOM_P$ intensities at stations M7-1 and M7-2 was insignificant relative to those at stations M6-1 and M8, although $FDOM_P$ is often used as a tracer of anthropogenic material including treated effluents (Hudson et al., 2007). Thus, we conclude that the concentration of DOC at station M7-1 was not influenced by STP. This STP appears to reduce TOC concentrations to a level that cannot influence the DOC concentrations resulting from the mixing of other sources, as shown in several other estuaries (Abril et al., 2002).

In general, anomalously high $FDOM_P$ was observed for anthropogenic sources (Coble, 1996; Baker et al., 2003). The δ^{13}C values of sewage effluents generally ranged from –22‰ to –28.5‰ (Andrews et al., 1998; Barros et al., 2010), and those of STP effluents ranged from –24‰ to –28‰ (Griffith et al., 2009). The δ^{13}C vs $FDOM_P$ plot (Fig. 3.7b) shows that there was no increase in $FDOM_P$ for samples which had depleted δ^{13}C values. Thus, we conclude that there was no significant DOC input from

urban/sewage or STP sources of DOC in this bay.

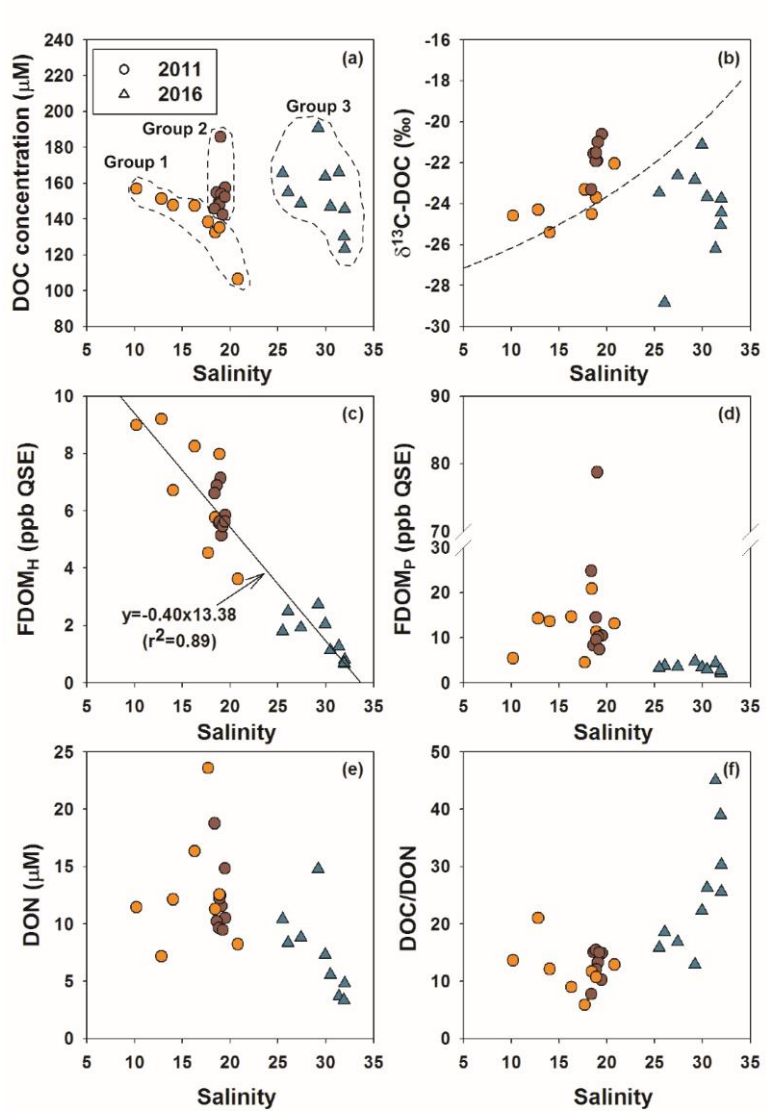

Figure 3.6. Relationships between salinity versus (a) DOC, (b) δ^{13}C-DOC, (c) $FDOM_H$, (d) $FDOM_P$, (e) DON, and (f) DOC/DON values. The DOC concentrations are divided into three groups based on probable different sources (in the dashed circles). The dashed line (b) represents the binary conservative mixing line for δ^{13}C-DOC between the terrestrial end-member and the marine end-member. The solid line (c) represents a linear regression fit of the data.

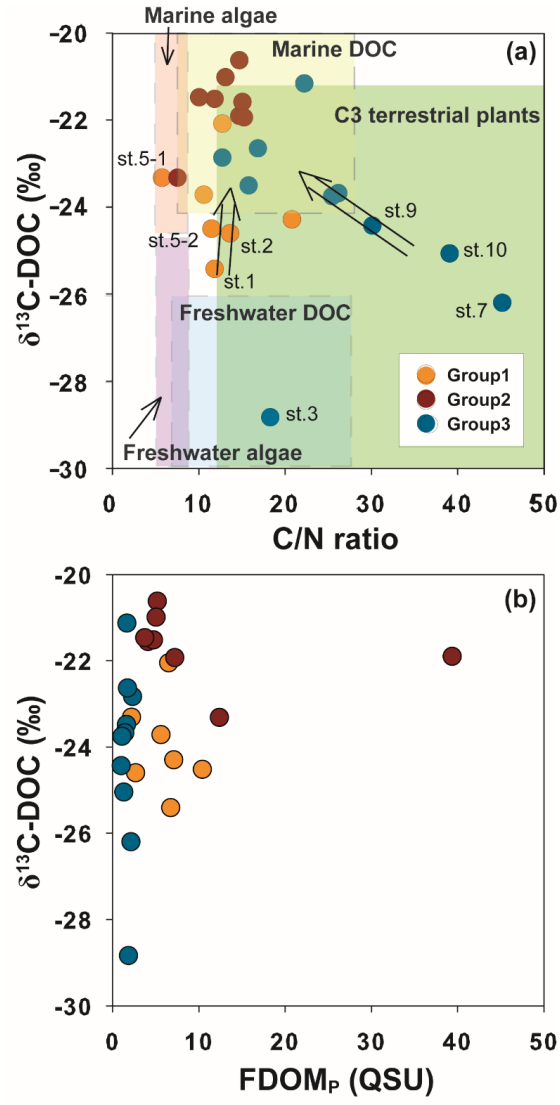

Figure 3.7. Relationships between δ^{13}C-DOC versus (a) DOC/DON ratio and (b) $FDOM_P$ in Masan Bay. The ranges of DOC/DON ratios and δ^{13}C-DOC values are based on the values reported by Lamb et al. (2006) and Beaupré (2015).

4. Sources, fluxes, and behaviors of fluorescent dissolved organic matter (FDOM) in the Nakdong-River Estuary, Korea

4.1 Introduction

Generally, DOC includes FDOM, which emits fluorescent light due to its chemical characteristics. As FDOM accounts for 20–70% of the DOC in coastal waters (Coble, 2007) and controls the penetration of harmful UV radiation in the euphotic zone, it plays a critical role in carbon cycles as well as biological production. In addition, FDOM is known as a powerful indicator of humic and protein-like substances (Coble, 2007) in coastal waters. River discharge is generally the main source of humic-like FDOM in coastal waters, although it is also produced through *in situ* microbial activity (Romera-Castillo et al., 2011). In contrast, protein-like FDOM is known to be from biological production as well as anthropogenic sources (Baker and Spencer, 2004). Terrestrial humic substances behave conservatively in coastal areas due to their refractory characteristics (Del Castillo et al., 2000), whereas protein substances behave non-conservatively in many estuaries due to their relatively rapid production and degradation (Vignudelli et al., 2004). Since FDOM has significant impacts on carbon cycle and biogeochemistry in coastal waters, it is important to determine their sources and fluxes and behaviors in the estuarine mixing zone. While there are many attempts to estimate of riverine DOC flux (Burns et al., 2008; Bianchi et al., 2004; Dai et al., 2012),

evaluation of dynamic seasonal changes in DOC and FDOM flux is poorly quantified.

In this study, we analyzed DOC, δ^{13}C-DOC, and FDOM in estuarine water samples collected monthly from the Nakdong-River Estuary. Sampling was conducted at a fixed platform, which has been utilized for monitoring various environmental parameters. This sampling station is advantageous because we can collect water samples for a wide range of salinities throughout tidal fluctuations. Using the data obtained from this unique station, we were able to determine (1) the behaviors of DOM in the estuarine mixing zone, (2) the fluxes of DOM from rivers based on the slopes between salinities and DOM components, and (3) the changes in DOM sources using δ^{13}C-DOC in the estuarine samples. The slope measurement in the mixing zone may represent the endmember of DOM components in rivers better than site-specific measurements in the river, by integrating larger spaces and times.

4.2 Study area and sampling

4.2.1 Study area

The Nakdong-River Estuary, which is the estuary of the longest river in Korea, is a major source of water supplying the needs for drinking, agriculture, and industry. The main channel of Nakdong River is approximately 510 km in length with a watershed area of approximately 23,380 km^2. It faces the south-eastern coastal area of the Korean peninsula, passing through Busan which is the second largest city in Korea. The mean annual precipitation is 1150 mm, and most precipitation (60–70%) occurs during the summer monsoon and typhoon seasons (Jeong et al., 2007). To manage water supply and saltwater intrusion, estuary dams were constructed in the mouth of the river in 1987.

4.2.2 Sampling

Water samples were collected at the sampling site which is located 560 m downstream from the dam (Fig. 4.1). The sampling period was from October 2014 to August 2015. The 2-L water sampling was conducted every hour for 24 hours during spring tide using an auto-sampler (RoboChem^{TM} Autosampler, Model S3-1224N, Centennial Technology, Korea), with a depth of the water intake 1 m below the surface. After samples were collected in acid-cleaned polyethylene bottles, they were moved to the laboratory within 24 hours. All water samples were filtered using pre-combusted GF/F filters. The FDOM samples were stored in pre-combusted amber glass vials and kept below 4°C in a refrigerator before analysis. The DOC and δ^{13}C-DOC samples were acidified to pH ~2 using 6 M HCl to avoid bacterial activities and stored in pre-combusted glass ampoules. Ampoules were fire-sealed to prevent the samples from any contaminations. The samples were analyzed for DOC and CDOM within a week. Salinity was measured using a YSI Pro Series conductivity probe sensor in the laboratory. The real-time and compulsory discharge volume data from the dam are available at http://www.water.or.kr, provided by K-Water. The monitoring program at this station is maintained by Korea Environment Management Corporation (KOEM). The water temperature data are recorded automatically at the site. The data are available at https://www.koem.or.kr.

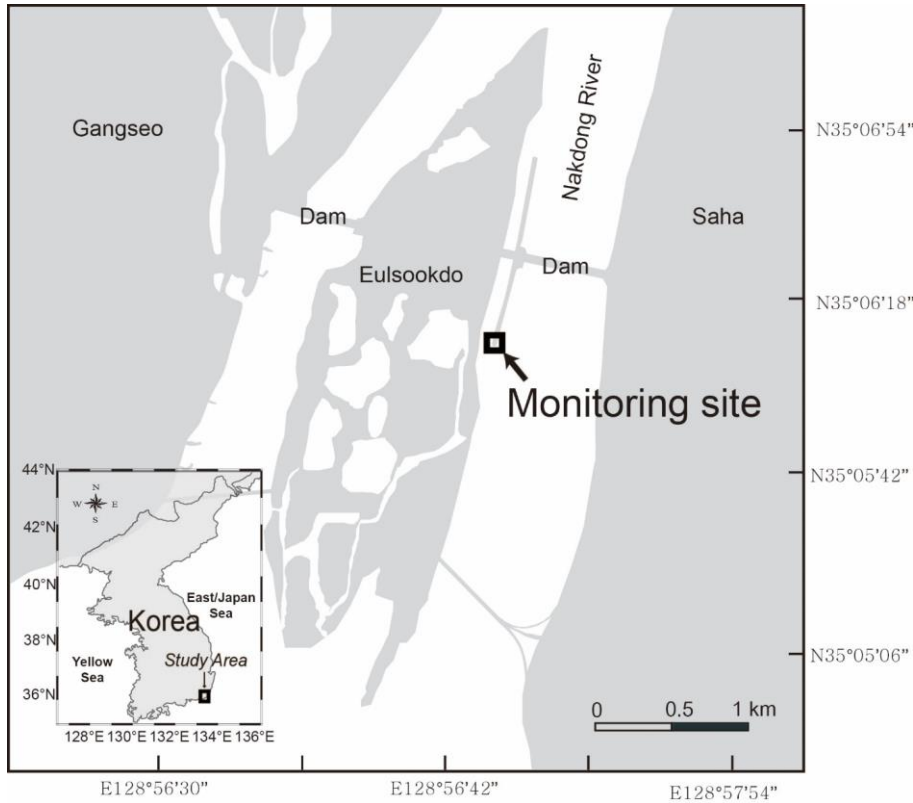

Figure 4.1. Map of the Nakdong-River Estuary. The square indicates a fixed monitoring site, located 560 m downstream from the dam.

4.3 Results and discussion

Salinities ranged from 0.1 to 28.5 over the sampling period of a year. Salinities in the sampling location were dependent primarily on the volume of river-water discharge from the dam. The volumes of river discharge were relatively larger in October, April, July, and May. The mean annual surface water temperature was 16°C, with the lowest temperature (avg. 8°C) in December and the highest temperature in August (avg. 26°C).

4.3.1 Behaviors and sources of DOC in the estuarine mixing zone

The concentrations of DOC ranged from 100 to 300 μM, with the highest concentrations in July (avg. 243 μM) and the lowest concentrations in February (avg. 115 μM), consistent with the typical DOC concentration ranges in coastal waters (Wang et al., 2004; Raymond and Bauer, 2001). The concentrations of DOC correlated significantly with salinities (r^2 = 0.59–0.92, $p < 0.0001$), indicating that DOC behaves conservatively in the mixing zone of this estuary (Fig. 4.2A), which is commonly observed in estuarine mixing zones (Laane, 1980; Mantoura and Woodward, 1983; Del Castillo et al., 2000; Clark et al., 2002; Jaffé et al., 2004).

If the high salinity periods are excluded, both the slope and y-intercept of DOC concentrations versus salinities were highest in July (Fig. 4.2), which could be due to a higher terrestrial DOC loading in the summer period, as observed in Horsens Fjord, Denmark (Markager et al., 2011). For this comparison, we excluded the high-salinity

periods (> 20), including December, January, February, and June, since they showed a narrow and low DOC concentration range (103–163 μM), resulting in large uncertainties by extrapolating them to the fresh water.

The carbon isotope values in the Nakdong-River Estuary ranged from −28.2‰ to −17.6‰. In order to determine the source of DOC in fresh water, we plotted δ^{13}C-DOC values against salinities (Fig. 4.2B). The conservative mixing curve of δ^{13}C values can be obtained using the two endmember mixing equation (Spiker, 1980; Raymond and Bauer, 2001):

$$\delta^{13}C_s = \frac{F_r \delta^{13}C_r [DOC]_r + (1-F_r) \times \delta^{13}C_m [DOC]_m}{[DOC]_s} \quad \text{equation (1)}$$

where $\delta^{13}C_s$, $\delta^{13}C_r$ and $\delta^{13}C_m$ are the δ^{13}C-DOC values at a given sample salinity, river endmember salinity, and marine endmember salinity, respectively; F_r is the riverine freshwater fraction calculated from the measured salinities; $[DOC]_s$ and $[DOC]_m$ are the DOC concentrations at a given salinity and marine endmember salinity, respectively; $[DOC]_r$ is the endmember DOC value for the river water (Fig. 4.2).

The riverine DOC endmember values (S = 0) ranged from 174 to 284 μM. The marine endmember value (S = 29) of DOC is 100 μM with the δ^{13}C-DOC value of −19‰. If these values from each month are applied, the δ^{13}C-DOC endmember values for the river water extrapolated to be from −27.5 to −24.5‰ (average: −26.2‰). Overall, the carbon isotope values of our samples are fitted well into the conservative mixing curve of the overall trend, with a slight change using different endmember values for different

months (Fig. 4.2B). In general, δ^{13}C-DOC values range from −22 to −18‰ for marine phytoplankton, from −34‰ to −23‰ for terrestrial C3 plants, and from −16‰ to −10‰ for terrestrial C4 plants (Gearing 1988; Clark and Fritz, 1997). Carbon isotope values in our study confirm that the main source of DOC in the estuarine mixing zone is dominantly from terrestrial C3 plants over all seasons. However, the value was heavier at lower salinity ranges (S < 10) in March and April samples, perhaps in association with the higher biological production in the river.

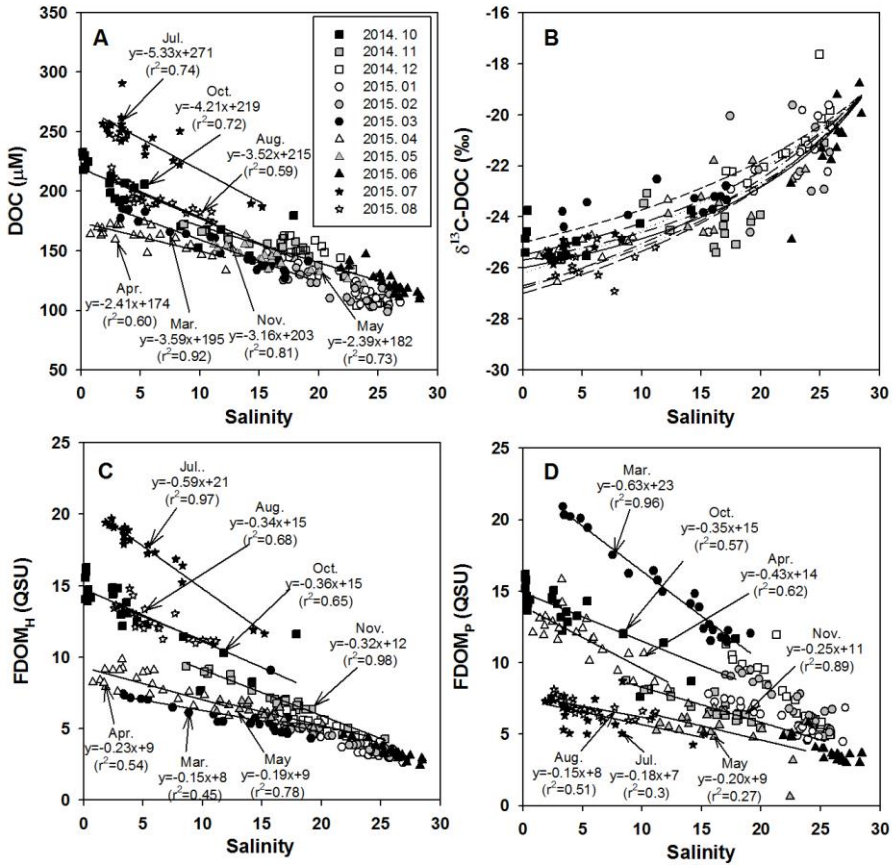

Figure 4.2. Salinities versus the concentrations of (A) DOC, (B) δ^{13}C-DOC, (C) $FDOM_H$, and (D) $FDOM_P$. The values for the regression lines are excluded for high-salinity periods (>20), including December, January, February, and June, which have large uncertainties in extrapolation. The solid curve (B) is the average conservative mixing line for the two endmember mixing equation. The dotted lines represent the monthly changes in mixing lines for the different monthly endmember values.

4.3.2 Behaviors and sources of FDOM in the estuarine mixing zone

Three components were identified in the water samples from the EEMs dataset. Based on the excitation-emission peak location, Component 1 ($FDOM_H$, Ex/Em = 320/418 nm) is found to be a terrestrial humic-like component (C peak) shown by Coble (2007). Component 2 ($FDOM_P$, Ex/Em = 280/328 nm) is found to be a tryptophan-like component (T peak), which is produced by microbial processes. Component 3 (Ex/Em = 300,325/364 nm) is found to be a marine humic-like component (M peak). Since Component 3 values were significantly correlated with Component 1 ($r^2 = 0.95$) values, we simply focused on Component 1 ($FDOM_H$) and Component 2 ($FDOM_P$) for data interpretations.

The concentrations of $FDOM_H$ ranged from 2.4 to 19.7 quinine sulfate unit (QSU), with the highest concentration in July (avg. 17.6 QSU) and the lowest concentration in June (avg. 3.4 QSU) (Fig. 4.2C). The concentrations of $FDOM_P$ ranged from 0.6 to 22.4 QSU, with the highest concentration in March (avg. 15.1 QSU) followed by October (avg. 13.6 QSU) (Fig. 4.2D).

The concentrations of both FDOM components were significantly correlated with salinities ($r^2 = 0.42–0.98$, $p < 0.0001$ for $FDOM_H$ and $r^2 = 0.27–0.96$, $p < 0.0001$ for $FDOM_P$), indicating that they are conservative in the mixing zone (Fig. 4.2). The slopes of $FDOM_H$ and $FDOM_P$ for each month ranged from −0.15 to −0.59 and −0.15 to −0.71, respectively. The higher $FDOM_H$ slopes in July and October were similar to the trend of DOC (Fig. 4.2C), which could be due to higher terrestrial FDOM production. However,

the seasons (March and April) in which higher $FDOM_P$ slopes occurred differ from those of DOC and $FDOM_H$, indicating that both FDOM components have different source inputs (Fig. 4.2D).

Although there are large differences in scattering of FDOM components against salinities, it is very difficult to compare scatterings for different seasons in order to discuss the different behaviors of DOM since the scattering is generally larger for the narrow salinity ranges. If the winter data are excluded, in March, during the highest biological production period in the river, the correlation coefficient against salinities was the highest for $FDOM_P$ and lowest for $FDOM_H$. In contrast, in June, during the highest fluvial DOM discharge period, the correlation coefficient against salinities was the highest for $FDOM_H$ and lowest for $FDOM_P$. This suggests that the biological production and removal, together with other generally known factors such as photo-degradation and sedimentary inputs, may affect the scattering of these FDOM components in the estuarine mixing zone.

As such, there was a significant positive correlation between $FDOM_H$ and DOC concentrations throughout all sampling periods ($r^2 = 0.93$, $p < 0.0001$) (Fig. 4.3A), suggesting that the main source of $FDOM_H$ and DOC is terrestrial based on $\delta^{13}C$-DOC values. Since FDOM does not usually contribute to a major portion of DOC, a positive correlation between FDOM and DOC has only been observed in specific areas, such as river-estuarine systems (Del Vecchio and Blough, 2004; Coble, 2007). Stedmon et al., (2006) demonstrated that stronger correlations were observed between DOC and FDOM

as humic substances derived from terrestrial DOM are more colored than DOM produced *in situ*. In general, terrestrial DOM occurring in rivers originates mainly from plant decomposition and leaf litter in the form of humic substances (Huang and Chen, 2009). As such, Gueguen et al., (2006) showed that humic materials are more effectively leached from soils during August and September under high temperatures. Thus, higher $FDOM_H$ slopes in August, October, and November, relative to the other periods, could be associated with higher terrestrial inputs of degradation products of soil organic matter (Dowell, 1985; Qualls et al., 1991).

In the study region, $FDOM_P$ concentrations were poorly correlated with DOC concentrations ($r^2 = 0.11$) (Fig. 4.3B). The slopes of $FDOM_P$ concentrations against DOC concentrations varied significantly over different seasons, with steeper gradients in the spring (March and April) and fall (October). In general, $FDOM_P$ is known to be produced efficiently by biological production in water (Coble, 1996; Belzile et al., 2002; Steinberg et al., 2004; Zhao et al., 2017). Thus, higher $FDOM_P$ concentrations, relative to DOC concentrations, in the spring and fall seems to be associated with the spring and fall phytoplankton blooms in river waters (Mayer et al., 1999; Zhang et al., 2009).

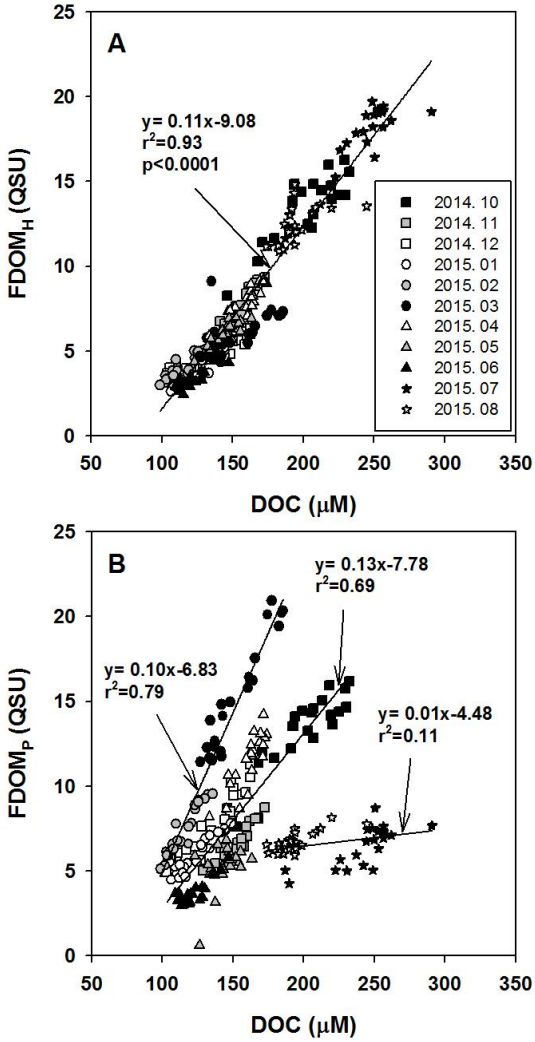

Figure 4.3. The plots of the concentrations of DOC versus the concentrations of (A) $FDOM_H$ and (B) $FDOM_P$.

4.3.3 Fluxes of DOC and FDOM in the estuarine mixing zone

The fluxes of DOC and FDOM from rivers to the ocean are calculated using the endmember values (C) of these components in rivers multiplied by the river discharge volumes (Q) for each month (Fig. 4.4). For this estimation, we assumed that (1) the endmember values are the same as the intercepts of the DOC, $FDOM_H$, and $FDOM_P$ versus salinity plots, and (2) the endmember values measured in the spring tides represent the concentrations of these components for each month.

River discharge was highest in April and July following heavy precipitation, and the largest discharge volume was about five-fold higher than that of winter discharges (Fig. 4.4A). However, the monthly variations of DOC endmember (y-intercept) values were quite constant, ranging from 174–284 μM. This indicates that the concentrations of DOC in the river are independent of river discharge volumes (Fig. 4.4B). The DOC endmember values were highest in December, followed by July and June (Fig. 4.4B). The monthly variation trend of $FDOM_H$ endmember values was similar to that of DOC, except for the December value. Excluding the December values, the $FDOM_P$ endmember values were highest in March, February, and October. These endmember trends are consistent with the slope variations explained in the previous section. Although there are large uncertainties in fresh water endmember values of DOC and FDOM in winter owing to narrow, high salinity ranges, we used the endmember values for the flux comparisons since the contribution of the uncertainties may be relatively small due to smaller river discharge volumes in winter.

The riverine DOC flux ranged from 1.6×10^6 mol day^{-1} (February) to 12.3×10^6 mol day^{-1} (July), indicating that there are large variations of DOC fluxes to the ocean. The riverine flux of $FDOM_H$ and $FDOM_P$ ranged from 1.4×10^9 QSU m^3 day^{-1} (December) to 23.1×10^9 QSU m^3 day^{-1} (July) and from 1.6×10^9 QSU m^3 day^{-1} (June) to 16.4×10^9 QSU m^3 day^{-1} (March), respectively. The seasonal variation trend of $FDOM_H$ was similar to that of DOC. The fluxes of $FDOM_P$ in December and March were twofold higher than those of $FDOM_H$ whereas the flux of $FDOM_H$ in July was 2–3 folds higher than that of $FDOM_P$. This shows that the fluxes of both components of FDOM differ significantly by seasons owing to the different source inputs even though their magnitudes are controlled mainly by river discharges.

It is well known that the single sampling event is not enough to capture the full range of natural variability in DOM abundance over all seasons (Stedmon et al., 2006; Huang and Chen, 2009; Markager et al., 2011; Dai et al., 2012; Moyer et al., 2015). Overall, our results show that monthly variations are significant. This implies that our understanding of DOC fluxes from large rivers is largely biased, depending on sampling resolution, methods, and hydrogeological settings of a specific river. For example, if summer data are extrapolated to annual river water discharge, the DOC and $FDOM_H$ fluxes can be overestimated up to three times for the Nakdong River.

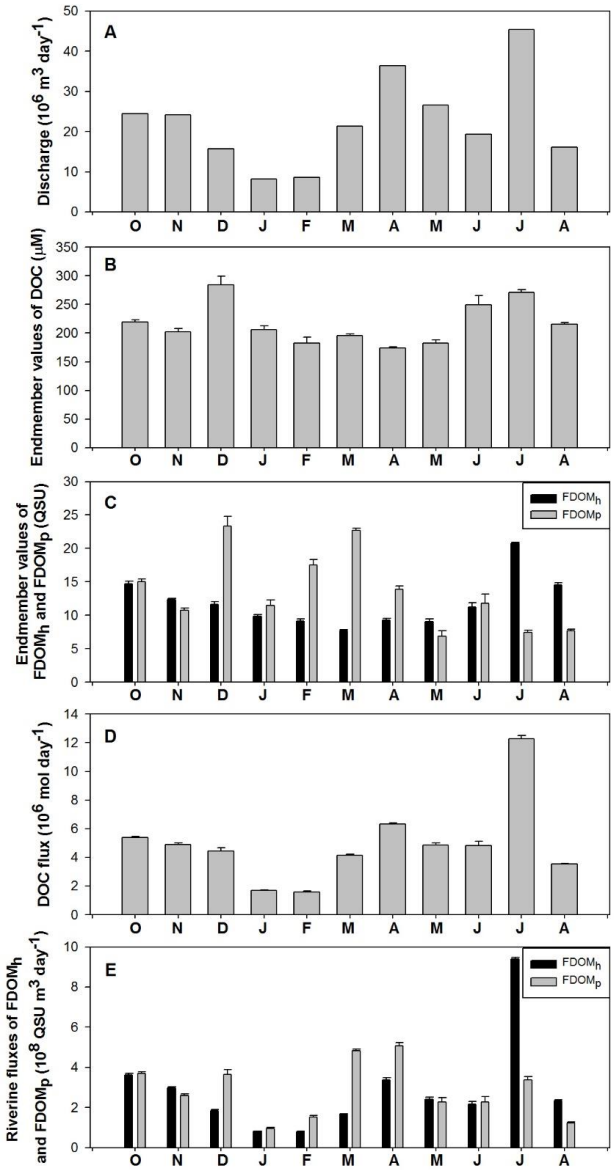

Figure 4.4. Temporal variations in discharge volumes, the endmember values of DOC, $FDOM_H$, and $FDOM_P$, and riverine fluxes of DOC, $FDOM_H$, and $FDOM_P$ in the Nakdong-River Estuary from October 2014 to August 2015.

5. Estimating net fluxes of dissolved organic matter and nutrients in coastal embayment using a radium tracer

5.1 Introduction

The main sources of DOC in coastal waters include terrestrial sources such as soil organic matter (OM) and degraded plant biomass (Hope et al., 1994; Benner and Opsahl, 2001; Raymond and Bauer, 2001), *in situ* production by phytoplankton and aquatic plants (Markager et al., 2011; Raymond et al., 2004), and anthropogenic sources (Griffith and Raymond, 2011). As such, nutrients in coastal waters originate from natural and anthropogenic sources. In addition, there are secondary nutrient inputs from bottom sediments and suspended particulate matter by microbial regeneration and from nitrogen fixation.

In the coastal zone, as a very dynamic realm of the marine environment, DOM and nutrients undergo various physical-chemical activities including modification, cycling, removal, and accumulation. The DOC in coastal waters is removed by microbial utilization and degradation (Moran et al., 1999; Raymond and Bauer, 2000), photo-oxidation (Moran and Zepp, 1997; Opsahl and Zepp, 2001), and absorption to suspended matter (Druffel et al., 1996). Nutrients in coastal areas consumed by biological activity thus remnant reaches the open ocean. Large nutrients fluxes often result in coastal eutrophication and harmful algal blooms.

The fluxes of DOM and nutrients from land to the ocean through rivers and groundwater have been extensively studied (Hope et al., 1994; Burns et al., 2008; Dai et al., 2012; Lee and Kim, 2018). In the river-dominated coastal areas, river-water discharge and biogeochemical reactions in estuaries control the fluxes of land-source fluxes to the ocean. In addition, submarine groundwater discharge (SGD) may happen along the entire coastal waters (Kim et al., 2012; Kim et al., 2013). Thus, the fluxes of DOM and nutrients through SGD often exceed those through rivers over basin-scale studies (Kim et al., 2013; Cho et al., 2018). The sources from rivers, streams, precipitation, and groundwater further experience rigorous biogeochemical regions in coastal waters before entering the open ocean. The biogeochemical reaction is important particularly in embayment where the residence time of water is long. The eventual flux of DOM and nutrients from the coastal ocean also plays an important role in the biogeochemical cycling and ecosystems of the receiving open ocean.

Although riverine fluxes of DOC and nutrients have been studied over the last a few decades (Williams, 1968; Schlesinger and Melack, 1981), the other pathways of DOC and nutrients fluxes, including seawater-land interaction, submarine groundwater discharge, and atmospheric deposition, are poorly understood. Bianchi et al., (2009) proposed that the inputs of photochemically-altered DOC from bay may provide an additional organic carbon source for microbial food webs in the open ocean (northern Gulf of Mexico). Thus, it is important to evaluate the various inputs of terrestrial sources

of DOC and nutrients in coastal waters and subsequent fluxes of biogeochemically transformed DOC and nutrients from coastal to the remote ocean.

In this study, we aim at evaluating the sources and sinks of DOM and nutrients in coastal embayment which have different freshwater inputs, water residence times, and biological production. In addition, we determine the net fluxes of DOM and nutrients from coastal embayment to the open ocean which may be dependent on the source inputs and biogeochemical alteration inside bays over their water residence times. In order to achieve this goals, we analyzed DOC, DON, δ^{13}C-DOC, FDOM, nutrients (DIN and DIP) and Ra isotopes, ^{223}Ra (half-life 11.68 d), ^{224}Ra (half-life 3.64 d), and ^{226}Ra (half-life 1600yr), in surface water samples collected from three different bays (Gwangyang Bay, Suyoung Bay, and Ulsan Bay).

5.2 Study area and sampling

5.2.1 study area

Gwangyang Bay (GB) is located on the southern coast of Korea with a total area of approximately 230 km^2 (Fig. 5.1a). GB is 17 km wide and 9 km long, with an average depth of 5–20 m (Jang and Han 2011). It is semi-enclosed, surrounded by the Yeosu peninsula and Namhae Islands which include the major industrial cities, big ports, and steel mills. The bay water has become more eutrophic due to the rapid growth of industrialization and population since the 1970s (Jang and Han 2011; Kim et al. 2015).

Suyoung Bay (SB) is located on the southeast coast of Korea with an area of approximately 14 km^2 (Fig. 5.1b). SB is 12 km wide and 6 km long, with an average depth of 5–20 m and is widely open toward the southern sea of Korea. Topography has a gentle slope in the middle of the bay and is a steep slope in the eastern and western sides. The freshwater discharge from Suyoung River is approximately 185×10^6 t y^{-1} (5.8 m^3 s^{-1}). This bay includes popular beaches (Gwanganri beach and Heundae beach) and an international yachting center.

Ulsan Bay (UB), which is located on the eastern coast of Korea (Figure. 5.1c), is 3.2 km wide and 8.3 km long with an area of approximately 56.6 km^2. The average depth of the inner bay is approximately 10 m. The annual amount of freshwater discharge

from streams which include Taehwa River is approximately 464×10^6 t y^{-1} (Lee et al., 2005). This bay is surrounded by highly industrialized regions and the biggest industrial ports. Ulsan area has over 100 plants and a lot of industrial complexes and facilities, with a population of over 1 million people.

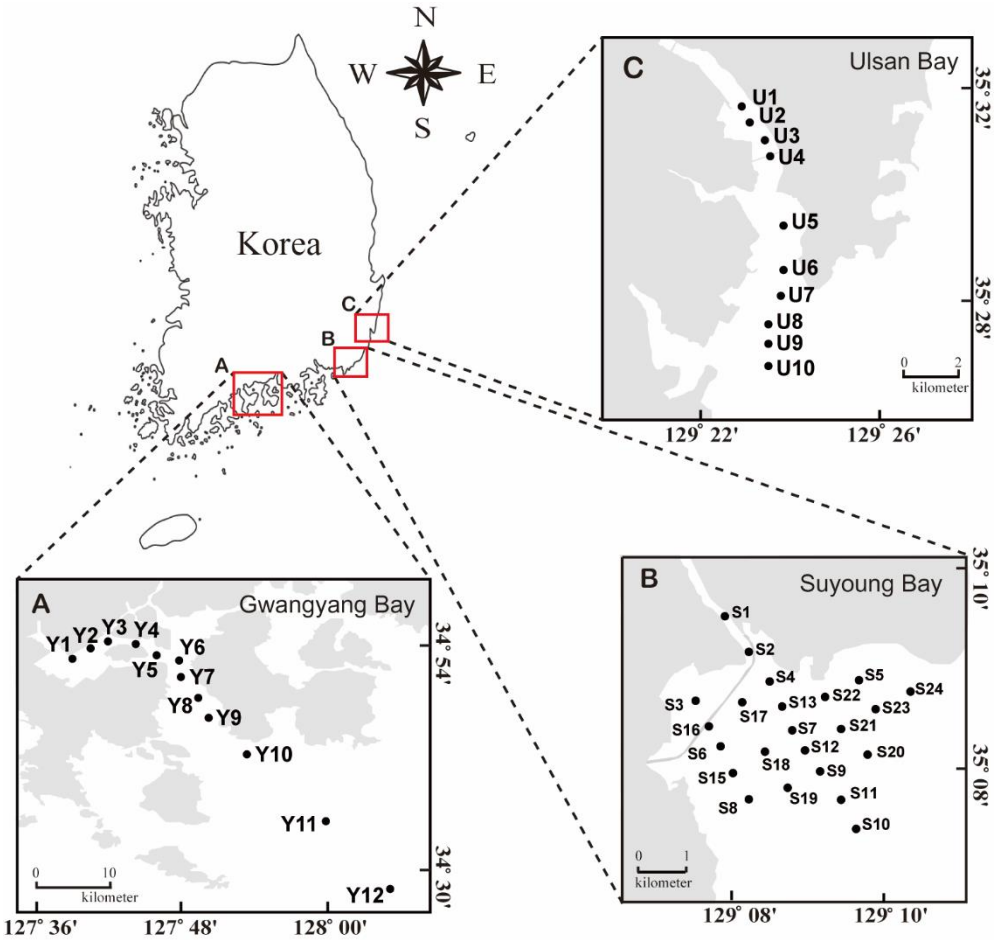

Figure 5.1. Maps of study areas in (A) Gwangyang Bay, (B) Suyoung Bay, and (C) Ulsan Bay on the southern-eastern coast of the Korean peninsula.

5.2.2 Sampling

Surface water samples of three bays (GB, UB, and SB) were collected from the inner bay to the outer bay sites (Fig. 5.1). The sampling was conducted at GB in March 2017, UB in August 2016, and SB in July 2017. The surface water samples of GB were collected using a rosette of 20 L Niskin bottle on board a ship (RV-NARA). The surface water samples of UB and SB were collected using a pump system from a small boat. At each sampling station, surface water samples were collected from ~0.5 m below the surface. All water samples were filtered through pre-combusted GF/F filter (0.45 μm pore size) or syringe filter (GF/F, Whatman) for DOC, δ^{13}C-DOC, FDOM, and nutrients analyses. Salinity and temperature in UB and SB were measured with a YSI meter at the field stations right after sampling, and salinity and temperature in GB were measured by CTD (SBE 911+).

Filtered samples for DOC and δ^{13}C-DOC were collected in pre-combusted glass ampoule and fire sealed after acidifying to pH 2 with 6M HCl. Filtered samples for FDOM analysis were collected in pre-combusted amber vials and stored in a refrigerator (below 4°C). For nutrients measurement, 50ml of filtered samples were stored in the conical tube and kept frozen until analysis. For ^{223}Ra, ^{224}Ra, and ^{226}Ra measurements, about 100L seawater was passed through an acrylic column which filled with 16 g (dry) of MnO_2-impregnated acrylic fiber (4.5 cm in diameter, 20 cm in length) with a flow rate of 1.0 L min^{-1} (Kim et al. 2001; Moore and Reid 1973).

5.3 Results

Salinities for surface water samples collected in GB ranged from 33 to 34, which were higher than those from other bays (Fig. 5.2 and 5.3). Although GB is often affected by Seomjin River discharge (Kang et al., 2003), the river water inputs were insignificant during the sampling period. The salinities of the surface water in the SB ranged from 30 to 34, except the lowest value (S=22) at the innermost station (S1) (Fig. 5.4). Salinities of the UB were in the range of 21.37–30.16, showing a gradual increase from the inner bay to the outer bay. Activities of ^{223}Ra and ^{226}Ra were in the range of 0.8–5.2 Bq/m^3 and 0.3–1.5 Bq/m^3, in GB, 1.1–2.5 Bq/m^3 and 11–31 Bq/m^3, in SB, and 0.1–1.9 Bq/m^3 and 0.6–20 Bq/m^3, respectively. Both isotopes showed higher activities near the shore and gradual decreases toward the outer bay, generally.

The concentrations of DOC in the three bays ranged from 64 μM to 325 μM, which fall into the DOC ranges commonly observed in coastal waters (Gao et al. 2010; Kim et al. 2012; Osburn and Stedmon 2011). Concentrations of DOC in GB (80–325 μM) were higher values than those in the other bays. In SB, the concentrations of DOC (64–170 μM) showed the highest value at the innermost bay (SY1). In UB, the concentrations of DOC (101–146 μM) showed a gradual decrease toward the outer bay (Fig. 5.2). The values of δ^{13}C-DOC ranged from −24.6‰ to −18.4‰ for the surface seawater samples throughout all bays (Fig. 5.2). In the outer bays, δ^{13}C-DOC values ranged from −21.2‰ to −19.9‰, which agree with the marine δ^{13}C value (−18 to −22‰)

(Fry et al. 1998). The concentrations of $FDOM_H$ in GB, SB, and UB were in the range of 0.8–1.6 R.U. (average 1.3 R.U.), 0.9–10.4 R.U. (average 1.7 R.U.), 3.3–6.7 ppb QSE (average 4.9 ppb QSE), respectively. The horizontal distribution patterns of $FDOM_H$ are opposite to those of salinities for all three bays.

The concentrations of DIN and DIP in GB were in the range of 0.1–1.6 μM and 0.01 to 0.1 μM, respectively, which were lower than the other bays. The concentrations of DIN in SB and UB were in the range of 5–229 μM and 1–23 μM, respectively. The concentrations of DIP in SB and UB were in the range of 0.2–8.6 μM and 0.01–2.6 μM, respectively. The concentrations of DON in GB and UB were in the range of 3.1–8.9 μM and 5–30 μM, respectively. The concentrations of DON in SB ranged from 0.7 to 13 μM, except the highest concentration (22 μM) at station S8.

We calculate the residence time of bay water using the pairs of ^{223}Ra and ^{224}Ra or ^{223}Ra and ^{226}Ra inventories. We assume that (1) the all "excess" activities of these two isotopes are from the innermost highest-activity stations, (2) there was no addition or removal of Ra inside the bay except the radioactive decays, and (3) the background of these two isotopes are from the open-ocean water (the lower activities observed in the outer bays). Then, the ages of total bay water can be calculated using the equation (2) for SB and UB and (3) for GB.

$$\left[\frac{\sum(\Delta^{224}Ra_n \times water\ mass_n)}{\sum(\Delta^{223}Ra_n \times water\ mass_n)}\right]_{inventory} = \left[\frac{\Delta^{224}Ra}{\Delta^{223}Ra}\right]_i \frac{e^{-\lambda_{224}t}}{e^{-\lambda_{223}t}} \qquad \text{equation (2)}$$

$$\left[\frac{\sum(\Delta^{228}Ra_n \times water\ mass_n)}{\sum(\Delta^{226}Ra_n \times water\ mass_n)}\right]_{inventory} = \left[\frac{\Delta^{228}Ra}{\Delta^{226}Ra}\right]_i \times e^{-\lambda_{228}t} \qquad \text{equation (3)}$$

where λ is the decay constant of ^{223}Ra (0.0608 day^{-1}), ^{224}Ra (0.1925 day^{-1}), and ΔRa_n value is calculated by subtracting the open-ocean endmember value from the measured, Ra_i is the initial activity of each isotope (the innermost highest activity subtracted for the open-ocean endmember value), and t is the age of the bay water. For the calculation of water mass at each station, the bay area was divided into each box. The maximum water depths in GB and UB were assumed to be 10 m, which is close to the mixed layer based on the measured CTD profile data. The maximum depth of SB was assumed to be 4 m, although CTD profile data are not available, by considering that sampling was performed in summer. Based on these assumptions, the average residence times of GB, SB, and UB were calculated to be 15, 1.9, and 1.5 days, respectively. We used the ^{223}Ra-^{226}Ra pair for GB since the residence time of water was older than 10 days based on the ^{224}Ra-^{223}Ra pair.

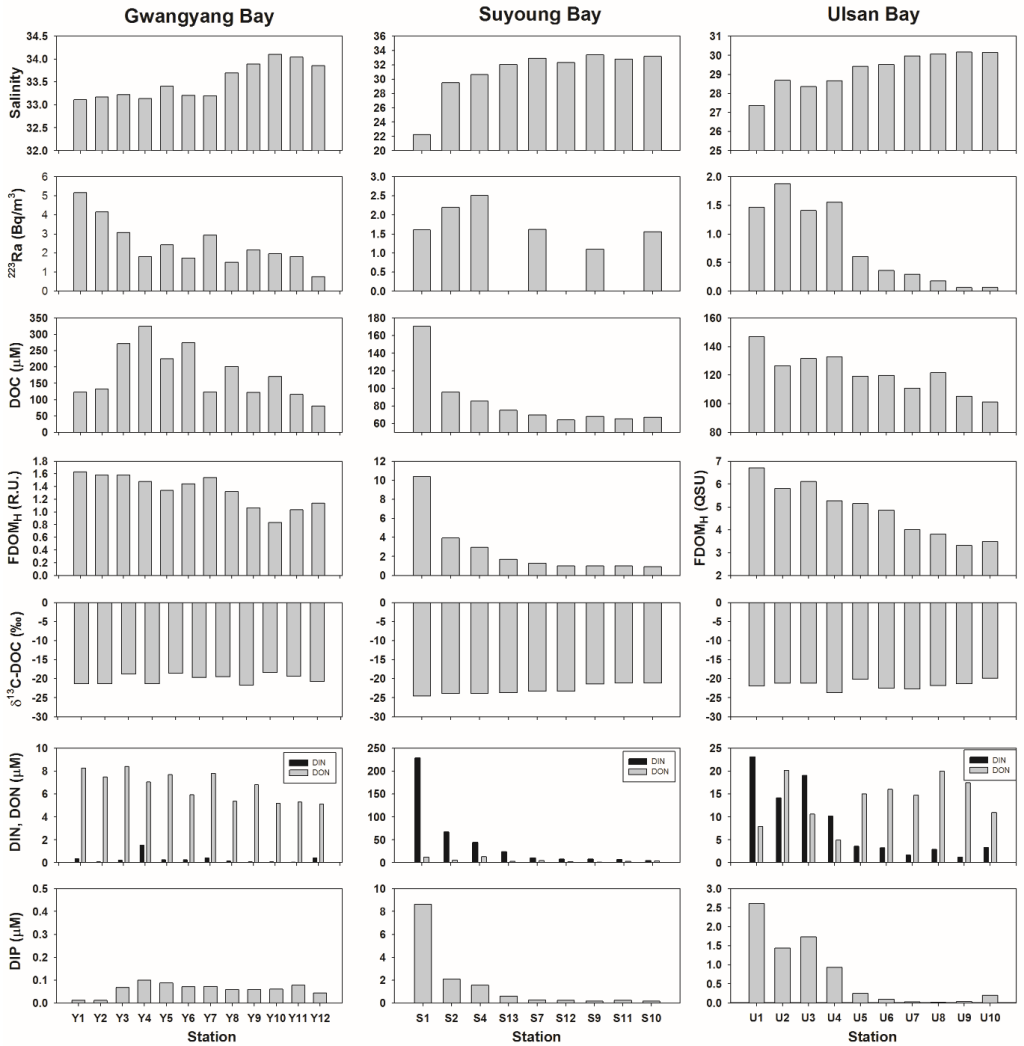

Figure 5.2. Distributions of salinity, ^{223}Ra, DOC, $FDOM_{H,}$ δ^{13}C-DOC, DIN, DON, and DIP in the surface waters of Gwangyang Bay, Suyoung Bay, and Ulsan Bay, Korea.

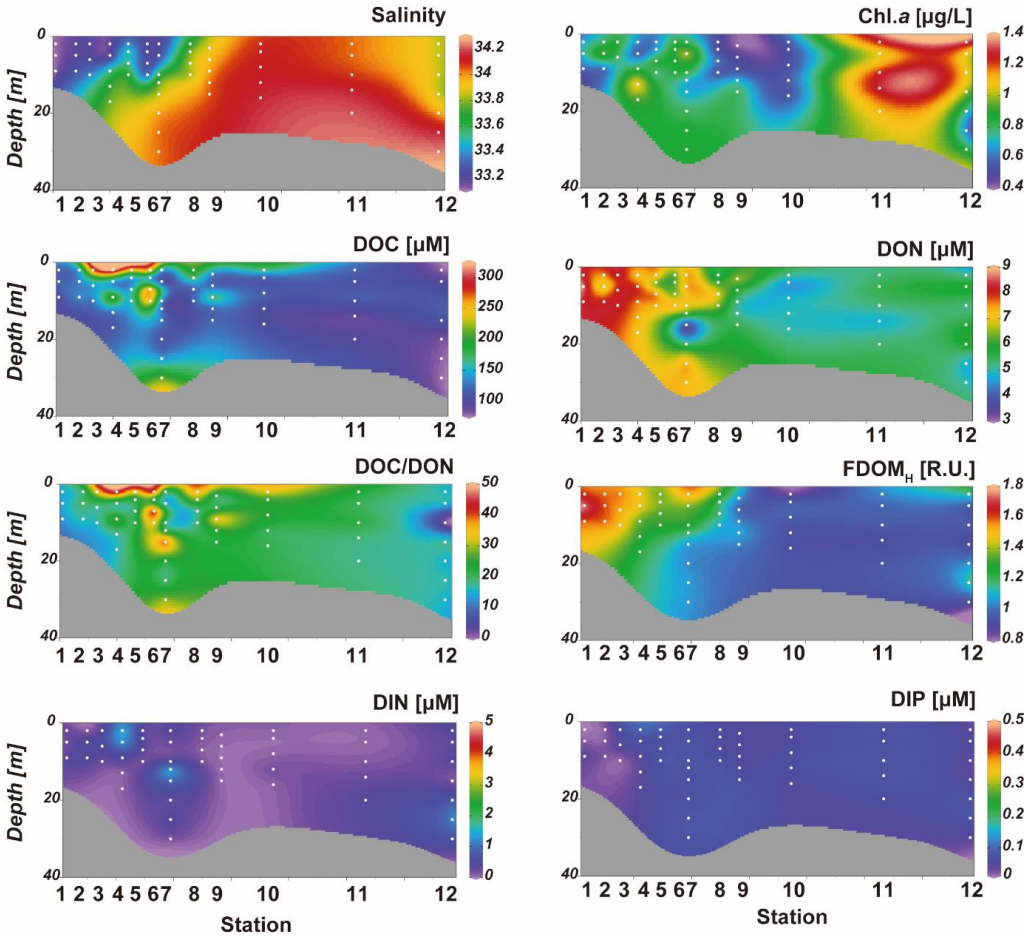

Figure 5.3. Vertical distributions of salinity, chlorophyll a, DOC, DON, DOC/DON, $FDOM_H$, DIN and DIP in Gwangyang Bay, Korea.

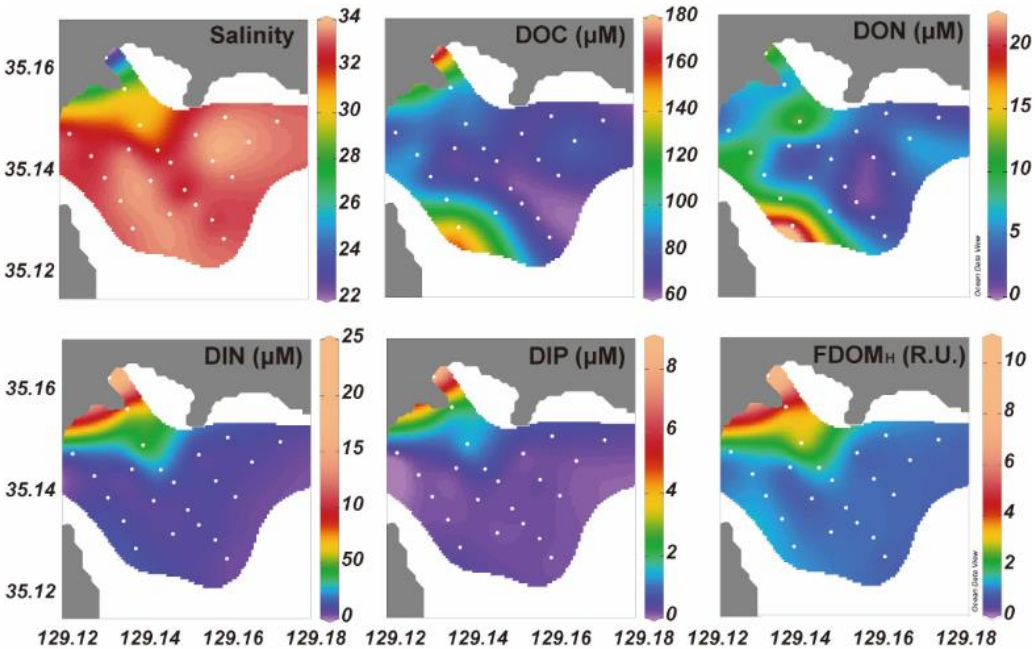

Figure 5.4. Horizontal distributions of salinity, DOC, DON, DIN, DIP, and $FDOM_H$ in Suyoung Bay, Korea.

5.4 Discussion

5.4.1 Factors controlling the distributions of DOC, FDOM, and nutrients

In UB, a linear correlation (r^2=0.87, P<0.0001) was observed between DOC and salinity (Fig. 5.5), indicating that DOC in freshwater (the extrapolated DOC concentration: 520 μM) is conservatively mixed with the open ocean water as commonly observed in many estuaries (Clark et al. 2002; Del Castillo et al. 2000; Jaffé et al. 2004). In SB and GB, the concentrations of DOC against salinities showed two different mixing patterns: The gentle slope showed a linear correlation between DOC and salinity, and there were significant increases in excess DOC in high salinity waters (Fig. 5.5). The gentle slope showed a linear correlation (r^2=0.99, P<0.0001 for SB; r^2=0.26, P=0.0005 for GB) between DOC and salinity (Fig. 5.5), indicating that DOC in freshwater (the extrapolated DOC concentration: 389 μM for SB and 914 μM for GB) is conservatively mixed with DOC in the open ocean. The excess DOC concentrations in SB and GB seem to be associated with extremely high production of DOC and/or anthropogenic sources.

$FDOM_H$ showed a significant linear relationship with salinity (r^2 = >0.92) in all bays which is commonly observed in coastal waters (Coble et al., 1998; Mayer et al., 1999; Guo et al., 2011) (Fig. 5.3). This trend indicates that humic substances that originate from terrestrial organic matter behave conservatively in coastal waters of all these bays (Coble et al., 1998; Mayer et al., 1999; Del Castillo et al., 2000). Therefore,

we preclude that the excess DOC observed in GB and SB is mostly non-humic substances.

In SB and UB, the concentrations of DIN and DIP showed a good correlation (r^2=0.91–0.97) with salinity, indicating that DIN and DIP concentrations behaved conservatively in these bays. Exceptionally higher concentrations of DIN and DIP were observed in SB (Fig. 5.6), perhaps associated with larger anthropogenic inputs from streams. In contrast, the concentrations of DIN and DIP in GB were depleted perhaps by biological consumption of both marine and terrestrial DIN and DIP. Higher concentrations of DIN and DIP were observed in the outer bay of GB (Fig. 5.7), supporting that nutrients influx from the outer bay was significantly consumed.

The concentrations of DON in SB showed lower concentrations than those of DIN except station 8, 15 and 16 where show DOC excess, suggesting that excess DON source at high salinity water in SB is related to excess DOC sources. DON concentrations in GB and UB showed much higher concentrations than DIN concentrations. At this stage, it is not clear whether or not the main source of DON is from terrestrial inputs or production in bay seawater.

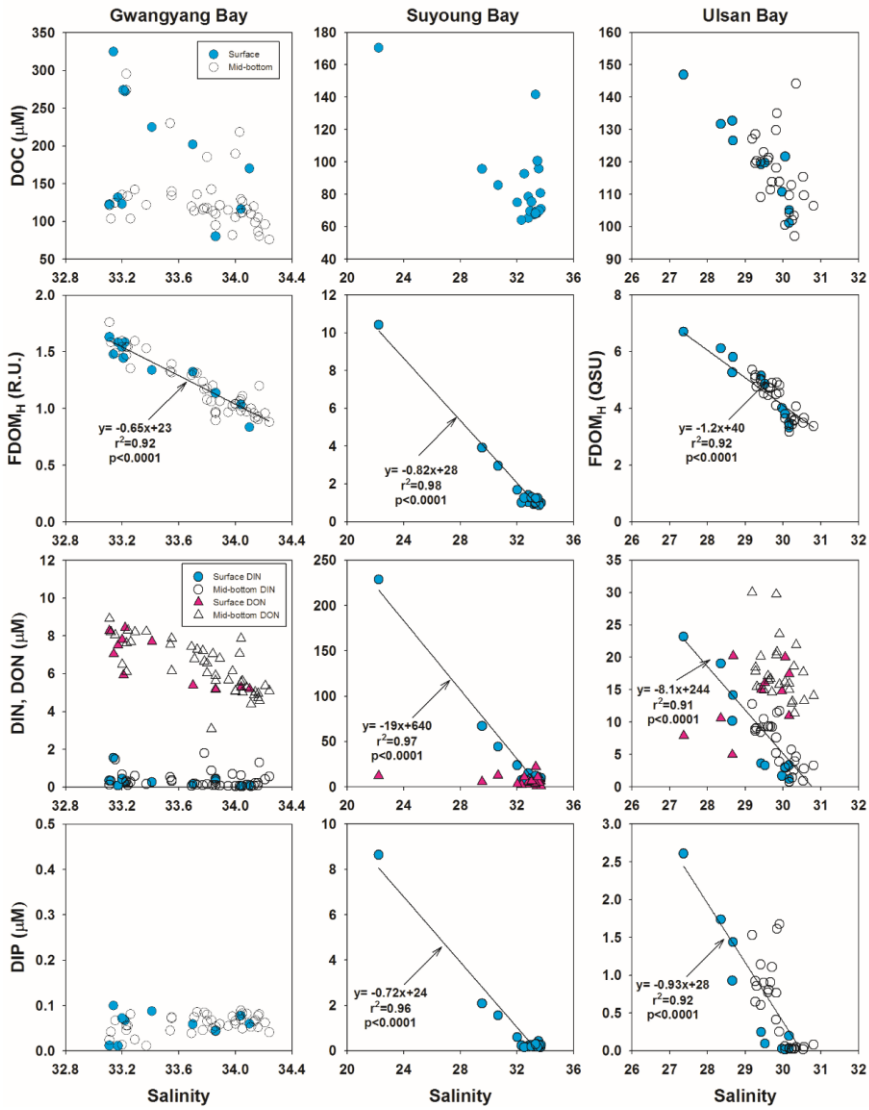

Figure 5.5. Plots of salinity versus DOC, $FDOM_H$, DIN, DON, and DIP in the seawaters of Gwangyang Bay, Suyoung Bay, and Ulsan Bay, Korea. The solid line is the conservative mixing line for the freshwater and open-ocean seawater mixing

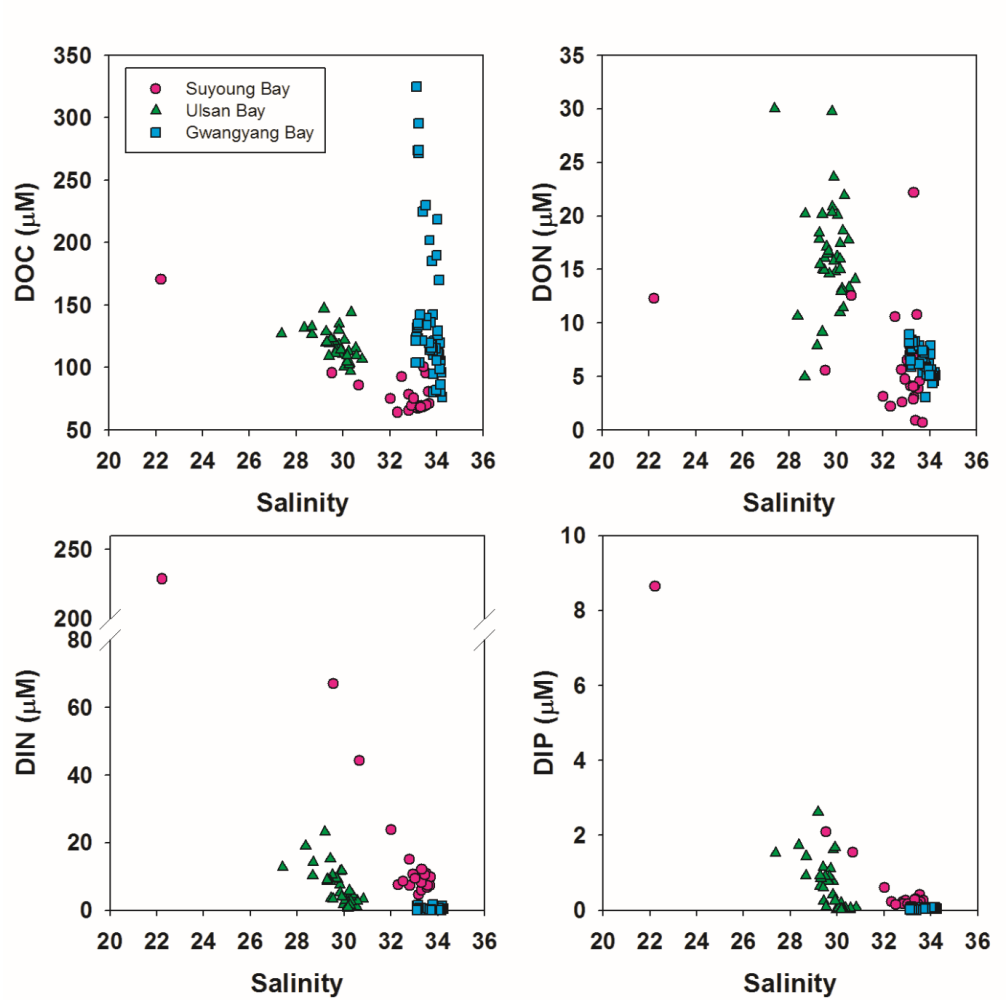

Figure 5.6. Plots of salinity versus DOC, DON, DIN, and DIP in the seawaters of Gwangyang Bay, Suyoung Bay, and Ulsan Bay, Korea.

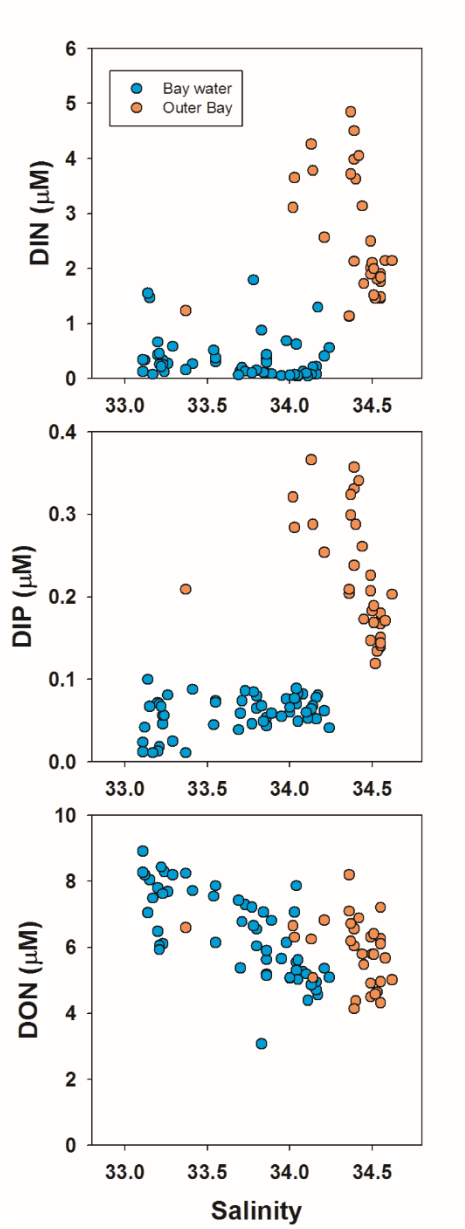

Figure 5.7. Plots of salinity versus DIN, DIP and DON in seawaters of Gwangyang Bay and outer bay.

5.4.2 Tracing DOC sources using δ^{13}C-DOC

In SB, based on DOC versus salinity plots, two different sources (Groups A and B) were identified. The δ^{13}C-DOC values of A group were generally fitted into the conservative mixing line between the freshwater (−27‰) and open-ocean water (−21‰), indicating that the higher DOC concentrations observed in lower salinity waters were from the Suyoung River source. The δ^{13}C-DOC values of B group ranged from −22.4‰ to −20.0‰, indicating that excess DOC concentrations in high-salinity waters are produced mainly by marine biological production. The δ^{13}C-DOC values in UB indicate that main DOC source in this bay is marine in origin (−22‰ to −18‰), with a slight influence of terrestrial C3 plants (−34‰ to −23‰,) (Deines, 1980; Kelley et al., 1998; Coffin and Cifuentes, 1999).

For GB, δ^{13}C-DOC values were within a narrow range of marine signals (–18‰ to –22‰) for salinity range of 33.11–34.10, although significant excess DOC was observed for high salinity waters (Fig. 5.5). Based on δ^{13}C-DOC values (Fig. 5.2), the source of the excess DOC in GB seems to be associated with high marine sources either by biological production or by anthropogenic activities. The maximum concentration of Chl. *a* was observed at station Y12, and no measurable increase was observed for higher DOC stations (Fig. 5.3). The ratios of DOC: DON for the stations increased up to 46 for higher DOC stations. Therefore, the main source of the excess DOC is unlikely from marine biological production. High DOC:DON ratio is typically associated with high age (Benner 2002) or terrestrial sources which are aromatic and high molecular mass DON

(McKnight and Aiken, 1998; Stepanauskas et al., 2002). DOC:DON ratios at the tidal flat were reported <25 (Kim et al., 2012) and those at fish farms reported 16-17 (Herbeck et al., 2013). High DOC: DON ratios for marine isotope values could be from marine sediment sources considering both the δ^{13}C-DOC values and C: N ratio, although we cannot confirm the source at this stage.

5.4.3 Estimation of DOC and nutrients fluxes using Ra box models

The flux of DOC from the bay to the open ocean can be calculated using the equation:

$$\text{CHEM flux} = \Sigma\left[(CHEM_i - CHEM_{outer)} \times V\ \right] \times \frac{1}{\tau} \qquad \text{equation (4)}$$

where DOC_i represents the concentration of DOC in the inner bay station, DOC_{Outer} represents the average concentration of DOC in the outer bay, V is the water volume (10^7 m^3) of each station, and τ is the residence time of bay water based on Ra isotopes (equation 2 and 3). This model assumes that (1) the mass balance of each component is at steady state, (2) the concentrations of each component in the outer bay water is conservative in the inner bay, and (3) removal of each component dissolved in seawater to the bottom sediment is negligible.

Total DOC flux in GB was estimated to be 36 × 10^5 mol/day, which is the highest value among the bays. The total DOC fluxes in SB and UB were 9 × 10^5 mol/day and 7 × 10^5 mol/day, respectively. Despite the absence of DOC inputs from freshwater, the total DOC flux to open ocean in GB is comparable with that of the Nakdong River (49 × 10^5 mol/day for water discharge volume of 2 × 10^7 m^3/day) (Lee and Kim, 2018). This result implies that the bay water which is not influenced by a large river can be an important DOC source, although the main source is not clearly identified in this study. A similar study conducted in the York River estuary suggests that in situ production of DOC can be equal or exceed the riverine origin (Raymond and Bauer, 2001).

DIN flux in SB was 50×10^4 mol/day which is the highest value than other bays where DIN flux in UB was 25×10^5 mol/day. DIP fluxes in SB and UB were 1.3×10^4 mol/day and 3×10^4 mol/day, respectively. If the freshwater volume is considered, the flux of nutrients from these bays are proportional to the Nakdong River. DIN and DIP flux in GB were not measurable because the difference of concentrations between the inner and outer bay is not significant. In fact, GB seems to be a sink of inorganic nutrients since DIN and DIP concentrations in the deeper water of the outer bay were higher than inner bay waters. In contrast, DON flux in GB was 20×10^4 mol/day, indicating that GB is a significant source of DON while it is a sink of DIN. These results suggest that biogeochemical alteration in the bay area plays an important role in the source and sink of DOM and nutrients resulting in a large impact on the fluxes to the open ocean.

Table 1. Characteristics of bays and calculated fluxes of freshwater, DOC, DON, DIN, and DIP in the Gwangyang Bay, Ulsan Bay, Suyoung Bay, and Nakdong river (Lee and Kim, 2018; Kim et al., 1996; Hong et al., 2000).

: not measurable because the difference of concentrations between the inner and outer bay is not significant

Region	Total area $10^7 m^2$	Avg. depth m	Residence time day	Freshwater flux $10^7 m^3$/day	DOC flux 10^5mol/day	DON flux 10^4mol/day	DIN flux 10^4mol/day	DIP flux 10^4mol/day
Gwangyang	13	10	14.6	0.15	36	20	-	-
Ulsan	1	10	1.5	0.22	7	-	25	3
Suyoung	1	4	1.9	0.16	9	-	50	1.3
Nakdong				2.2	49	111	881	17

6. Summary and conclusions

In the first section, the sources of DOM in Masan Bay were determined in 2011 and 2016 using the δ^{13}C-DOC, FDOM, and DOC/DON ratios. The main sources were separated into three groups based on DOC concentrations versus salinity plots. The DOM concentrations in the first group in 2011, which included the lowest salinity waters, were found to be mixtures of terrestrial DOM and open-ocean DOM sources based on the δ^{13}C values of −25.4‰ to −23.3‰ and a good correlation between $FDOM_H$ and salinity. The excess DOC concentrations in the second group in higher salinity waters in 2011 were found to be produced *in situ* by biological production based on more enriched δ^{13}C-DOC values (−22.0‰ to −20.6‰), high $FDOM_P$ concentrations, and low C/N ratios. The excess DOC concentrations in the third group in high salinity waters in 2016 seemed to be produced by direct interaction between land and seawater based on more depleted δ^{13}C-DOC values (−28.8‰ and −21.1‰), low FDOM concentrations, and high C/N ratios. This study shows that the combination of multiple DOM tracers, including δ^{13}C-DOC, FDOM, and DOC/DON ratios, is powerful for discriminating the complicated sources of DOM occurring in coastal waters.

In the Nakdong-River Estuary, the concentrations of $FDOM_H$ and DOC showed significant negative correlations against salinities throughout all sampling periods, indicating that they behave conservatively in this estuarine mixing zone. The slopes of both DOC and $FDOM_H$ concentrations versus salinities were highest in July, due to the largest terrestrial DOC loadings. The carbon isotope values showed that the main source of DOC in the estuarine mixing zone is terrestrial C3

plants over all seasons. The slopes of $FDOM_P$ versus salinity were relatively higher in March and April in association with the spring phytoplankton blooms in river and estuarine waters. The monthly fluxes of DOC, $FDOM_H$, and $FDOM_P$ showed large seasonal variations (5–10 folds), suggesting that the estimation of annual riverine fluxes of DOC, $FDOM_H$, and $FDOM_P$ requires careful considerations of seasonal changes in rivers.

In the final section, the relationship between DOC and salinity showed a different pattern in three bays (Gwangyang Bay, Suyoung Bay, and Ulsan Bay). In Ulsan Bay, a linear correlation was observed between DOC and salinity, indicating that DOC is mixed conservatively with seawater. In Suyoung Bay and Gwangyang Bay, two different mixing patterns are observed in the plot between DOC and salinity. In Suyoung Bay, one gentle slope is due to the conservative mixing between freshwater input and open ocean water whereas the other steep slope seems to be due to the production of phytoplankton based on the δ^{13}C-DOC values. In Gwangyang Bay, high concentration of DOC could be from marine dredged sediment sources considering both the δ^{13}C-DOC values and C: N ratio. Gwangyang Bay is a significant source of DOC and DON which is comparable amount with small rivers, but a sink of DIN and DIP. In contrast, Suyoung Bay and Ulsan Bay are determined to be the source of DIN and DIP to the outer bay. Thus, our study reveals that the residence times of coastal embayment play an important role in biogeochemical production and alteration of nutrients and DOM.

References

Abril, G., Nogueira, M., Etcheber, H., Cabeçadas, G., Lemaire, E., and Brogueira, M.: Behaviour of organic carbon in nine contrasting European estuaries, Estuarine Coastal Shelf Sci., 54, 241-262, 2002.

Andrews, J., A. Greenaway, and P. Dennis.: Combined carbon isotope and C/N ratios as indicators of source and fate of organic matter in a poorly flushed, tropical estuary: Hunts Bay, Kingston Harbour, Jamaica. Estuarine Coastal Shelf Sci. 46: 743-756, 1998.

Baker, A. and Inverarity, R.: Protein-like fluorescence intensity as a possible tool for determining river water quality, Hydrological Processes, 18, 2927-2945, 2004.

Baker, A. and Spencer, R. G.: Characterization of dissolved organic matter from source to sea using fluorescence and absorbance spectroscopy, Sci. Total Environ., 333, 217-232, 2004.

Balakrishna, K., I. A. Kumar, G. Srinikethan, and G. Mugeraya.: Natural and Anthropogenic Factors Controlling the Dissolved Organic Carbon Concentrations and Fluxes in a Large Tropical River, India. Environ. Monit. Assess. 122: 355-364, 2006.

Barros, G. V., L. A. Martinelli, T. M. O. Novais, J. P. H. Ometto, and G. M. Zuppi.: Stable isotopes of bulk organic matter to trace carbon and nitrogen dynamics in an estuarine ecosystem in Babitonga Bay (Santa Catarina, Brazil). Sci. Total Environ. 408: 2226-2232, 2010.

Bauer, J. E. and Bianchi, T. S.: Dissolved organic carbon cycling and transformation, in: Treatise on estuarine and coastal science, edited by: Wolanski, E.

and Mcluski, D. S., 5, 7-67, Academic Press, Waltham, 2011.

Bauer, J. E., Cai, W.-J., Raymond, P. A., Bianchi, T. S., Hopkinson, C. S., and Regnier, P. A.: The changing carbon cycle of the coastal ocean, Nature, 504, 61, 2013.

Beaupré, S. R.: Chapter 6 - The Carbon Isotopic Composition of Marine DOC, in: Biogeochemistry of Marine Dissolved Organic Matter (Second Edition), edited by: Hansell, D. A. and Carlson, C. A., Academic Press, Boston, 335-368, 2015

Belzile, C., Gibson, J. A., and Vincent, W. F.: Colored dissolved organic matter and dissolved organic carbon exclusion from lake ice: Implications for irradiance transmission and carbon cycling, Limnol. Oceanogr., 47, 1283-1293, 2002.

Benner, R.: What happens to terrestrial organic matter in the ocean? Mar. Chem. 92: 307-310, 2004.

Benner, R. and Opsahl, S.: Molecular indicators of the sources and transformations of dissolved organic matter in the Mississippi river plume, Org. Geochem., 32, 597-611, 2001.

Benner, R.: Chemical composition and reactivity, Biogeochemistry of marine dissolved organic matter, 3, 56-90, 2002.

Bianchi, T. S., DiMarco, S. F., Smith, R. W., and Schreiner, K. M.: A gradient of dissolved organic carbon and lignin from Terrebonne–Timbalier Bay estuary to the Louisiana shelf (USA), Mar. Chem., 117, 32-41, https://doi.org/10.1016/j.marchem.2009.07.010, 2009.

Bianchi, T. S., Filley, T., Dria, K., and Hatcher, P. G.: Temporal variability in sources of dissolved organic carbon in the lower Mississippi River, Geochim. Cosmochim. Acta, 68, 959-967, 2004.

Burns, K. A., Brunskill, G., Brinkman, D., and Zagorskis, I.: Organic carbon and

nutrient fluxes to the coastal zone from the Sepik River outflow, Cont. Shelf Res., 28, 283-301, 2008.

Carlson, C. A.: Chapter 4 - Production and Removal Processes in Biogeochemistry of Marine Dissolved Organic Matter edited by: Hansell, D. A. and Carlson, C. A., Academic Press, San Diego, 91-151, 2002.

Carlson, C. A., and Hansell, D. A.: Chapter 3 - DOM Sources, Sinks, Reactivity, and Budgets, in: Biogeochemistry of Marine Dissolved Organic Matter (Second Edition), edited by: Hansell, D. A., and Carlson, C. A., Academic Press, Boston, 65-126, 2015.

Cauwet, G.: Chapter 12 - DOM in the Coastal Zone, in: Biogeochemistry of Marine Dissolved Organic Matter, edited by: Hansell, D. A., and Carlson, C. A., Academic Press, San Diego, 579-609, 2002.

Cawley, K. M., Ding, Y., Fourqurean, J., and Jaffé, R.: Characterising the sources and fate of dissolved organic matter in Shark Bay, Australia: a preliminary study using optical properties and stable carbon isotopes, Mar. Freshwater Res., 63, 1098-1107, https://doi.org/10.1071/MF12028, 2012.

Chen, M., Kim, J.-H., Nam, S.-I., Niessen, F., Hong, W.-L., Kang, M.-H., and Hur, J. J. S. r.: Production of fluorescent dissolved organic matter in Arctic Ocean sediments, 6, 39213, 2016.

Chen, R. F., Bissett, P., Coble, P., Conmy, R., Gardner, G. B., Moran, M. A., Wang, X., Wells, M. L., Whelan, P., and Zepp, R. G.: Chromophoric dissolved organic matter (CDOM) source characterization in the Louisiana Bight, Mar. Chem., 89, 257-272, 2004.

Cho, H.-M., Kim, G., Kwon, E. Y., Moosdorf, N., Garcia-Orellana, J., and Santos, I. R.: Radium tracing nutrient inputs through submarine groundwater discharge in the

global ocean, Sci. Rep., 8, 2439, 2018.

Clark, C. D., Jimenez-Morais, J., Jones, G., Zanardi-Lamardo, E., Moore, C. A., and Zika, R. G.: A time-resolved fluorescence study of dissolved organic matter in a riverine to marine transition zone, Mar. Chem., 78, 121-135, 2002.

Clark, I.J. and Fritz, P.: Environmental Isotopes in Hydrogeology, CRC Press/Lewis Publishers, Boca Raton, 1997.

Coble, P. G., Del Castillo, C. E., and Avril, B.: Distribution and optical properties of CDOM in the Arabian Sea during the 1995 Southwest Monsoon, Deep Sea Research Part II: Topical Studies in Oceanography, 45, 2195-2223, 1998.

Coble, P. G., Green, S. A., Blough, N. V., and Gagosian, R. B.: Characterization of dissolved organic matter in the Black Sea by fluorescence spectroscopy, Nature, 348, 432, 1990b.

Coble, P. G.: Characterization of marine and terrestrial DOM in seawater using excitation-emission matrix spectroscopy, Mar. Chem., 51, 325-346, 1996.

Coble, P. G.: Marine optical biogeochemistry: the chemistry of ocean color, Chemical reviews, 107, 402-418, 2007.

Coffin, R. B., and Cifuentes, L. A.: Stable isotope analysis of carbon cycling in the Perdido Estuary, Florida, Estuaries, 22, 917-926, 1999.

Dai, M., Yin, Z., Meng, F., Liu, Q., and Cai, W.-J.: Spatial distribution of riverine DOC inputs to the ocean: an updated global synthesis, Curr. Opin. Environ. Sustainability, 4, 170-178, https://doi.org/10.1016/j.cosust.2012.03. 003, 2012.

Dalmagro, H. J., Lathuillière, M. J., Sallo, F. d. S., Guerreiro, M. F., Pinto, O. B., de Arruda, P. H., Couto, E. G., and Johnson, M. S. J. W.: Streams with Riparian Forest Buffers versus Impoundments Differ in Discharge and DOM Characteristics for Pasture Catchments in Southern Amazonia, 11, 390, 2019.

De Troyer, I., Bouillon, S., Barker, S., Perry, C., Coorevits, K., and Merckx, R.: Stable isotope analysis of dissolved organic carbon in soil solutions using a catalytic combustion total organic carbon analyzer-isotope ratio mass spectrometer with a cryofocusing interface, Rapid Commun. Mass Spectrom., 24, 365-374, 2010.

Deines, P.: The isotopic composition of reduced organic carbon, Handbook of environmental isotope geochemistry, 329-406, 1980.

Del Castillo, C. E., Gilbes, F., Coble, P. G., and Müller-Karger, F. E.: On the dispersal of riverine colored dissolved organic matter over the West Florida Shelf, Limnol. Oceanogr., 45, 1425-1432, 2000.

Del Vecchio, R., and Blough, N. V.: Spatial and seasonal distribution of chromophoric dissolved organic matter and dissolved organic carbon in the Middle Atlantic Bight, Mar. Chem., 89, 169-187, 2004.

Dowell, W. H.: Kinetics and mechanisms of dissolved organic carbon retention in a headwater stream, Biogeochemistry, 1, 329-352, 1985.

Druffel, E. R., Bauer, J. E., Williams, P. M., Griffin, S., and Wolgast, D.: Seasonal variability of particulate organic radiocarbon in the northeast Pacific Ocean, Journal of Geophysical Research: Oceans, 101, 20543-20552, 1996.

Faganeli, J., Malej, A., Pezdic, J., and Malacic, V.: C: N: P ratios and stable c-isotopic ratios as indicators of sources of organic-matter in the gulf of trieste (northern adriatic), Oceanolog. Acta, 11, 377-382, 1988.

Fisher, T. R., J. D. Hagy, and E. Rochelle-Newall.: Dissolved and particulate organic carbon in Chesapeake Bay. Estuaries 21: 215-229, 1998.

Fontugne, M., and J. Duplessy.: Organic-carbon isotopic fractionation by marine plankton in the temperature-range-1 to 31-degrees c. Oceanolog. Acta 4: 85-90, 1981.

Fry, B., Hopkinson, C. S., Nolin, A., and Wainright, S. C.: $^{13}C/^{12}C$ composition of marine dissolved organic carbon, Chem. Geol., 152, 113-118, 1998.

Gao, L., Fan, D., Li, D., and Cai, J.: Fluorescence characteristics of chromophoric dissolved organic matter in shallow water along the Zhejiang coasts, southeast China, Marine environmental research, 69, 187-197, 2010.

Gearing, J.N., The use of stable isotope ratios for tracing the nearshore–offshore exchange of organic matter. In: Jansson, B.-O. (Ed.), Coastal-Offshore Ecosystem Interactions, Springer-Verlag, Berlin, 69–101, 1988.

Griffith, D. R. and Raymond, P. A.: Multiple-source heterotrophy fueled by aged organic carbon in an urbanized estuary, Mar. Chem., 124, 14-22, 2011.

Griffith, D. R., Barnes, R. T., and Raymond, P. A.: Inputs of fossil carbon from wastewater treatment plants to US rivers and oceans, Environ. Sci. Technol., 43, 5647-5651, 2009.

Gueguen, C., Guo, L., Wang, D., Tanaka, N., and Hung, C.-C.: Chemical characteristics and origin of dissolved organic matter in the Yukon River, Biogeochemistry, 77, 139-155, 2006.

Guo, L., and P. H. Santschi.: Isotopic and elemental characterization of colloidal organic matter from the Chesapeake Bay and Galveston Bay. Mar. Chem. 59: 1-15, 1997.

Hansell, D. A. and C. A. Carlson: Biogeochemistry of Marine Dissolved Organic Matter. Academic Press, San Diego, 774 pp. 2002.

Hedges, J. I., Cowie, G. L., Richey, J. E., Quay, P. D., Benner, R., Strom, M., and Forsberg, B. R.: Origins and processing of organic matter in the Amazon River as indicated by carbohydrates and amino acids Limnol. Oceanogr., 39, 743-761, 1994.

Hedges, J. I.: Global biogeochemical cycles: progress and problems, Mar. Chem.,

39, 67-93, 1992.

Herbeck, L. S., Unger, D., Wu, Y., and Jennerjahn, T. C.: Effluent, nutrient and organic matter export from shrimp and fish ponds causing eutrophication in coastal and back-reef waters of NE Hainan, tropical China, Cont. Shelf Res., 57, 92-104, 2013.

Hong, S. H., Kannan, N., Jin, Y., Won, J. H., Han, G. M., and Shim, W. J.: Temporal trend, spatial distribution, and terrestrial sources of PBDEs and PCBs in Masan Bay, Korea, Mar. Pollut. Bull., 60, 1836-1841, 2010.

Hope, D., Billett, M., and Cresser, M.: A review of the export of carbon in river water: fluxes and processes, Environ. Pollut., 84, 301-324, 1994.

Huang, W., and Chen, R. F.: Sources and transformations of chromophoric dissolved organic matter in the Neponset River Watershed, Journal of Geophysical Research: Biogeosciences, 114, 2009.

Hudson, N., Baker, A., and Reynolds, D.: Fluorescence analysis of dissolved organic matter in natural, waste and polluted waters—a review, River Research and Applications, 23, 631-649, 2007.

Jaffé, R., Boyer, J., Lu, X., Maie, N., Yang, C., Scully, N., and Mock, S.: Source characterization of dissolved organic matter in a subtropical mangrove-dominated estuary by fluorescence analysis, Mar. Chem., 84, 195-210, 2004.

Jang, J., and Han, S.: Importance of monsoon rainfall in mass fluxes of filtered and unfiltered mercury in Gwangyang Bay, Korea, Sci. Total Environ., 409, 1498-1503, 2011.

Jeong, K.-S., Kim, D.-K., and Joo, G.-J.: Delayed influence of dam storage and discharge on the determination of seasonal proliferations of Microcystis aeruginosa and Stephanodiscus hantzschii in a regulated river system of the lower Nakdong

River (South Korea), Water Res., 41(6), 1269-1279, 2007.

Jiao, N., Herndl, G. J., Hansell, D. A., Benner, R., Kattner, G., Wilhelm, S. W., Kirchman, D. L., Weinbauer, M. G., Luo, T., and Chen, F.: Microbial production of recalcitrant dissolved organic matter: long-term carbon storage in the global ocean, Nat. Rev. Microbiol., 8, 593-599, 2010.

Kang, C.-K., Kim, J. B., Lee, K.-S., Kim, J. B., Lee, P.-Y., and Hong, J.-S.: Trophic importance of benthic microalgae to macrozoobenthos in coastal bay systems in Korea: dual stable C and N isotope analyses, Mar. Ecol. Prog. Ser., 259, 79-92, 2003.

Kannan, N., Hong, S. H., Yim, U. H., Kim, N. S., Ha, S. Y., Li, D., and Shim, W. J.: Dispersion of organic contaminants from wastewater treatment outfall in Masan Bay, Korea, Toxicology and Environmental Health Sciences, 2, 200-206, 2010.

Kelley, C. A., Coffin, R. B., and Cifuentes, L. A.: Stable isotope evidence for alternative bacterial carbon sources in the Gulf of Mexico, Limnol. Oceanogr., 43, 1962-1969, 1998.

Kim, G., Burnett, W., Dulaiova, H., Swarzenski, P., and Moore, W.: Measurement of 224Ra and 226Ra activities in natural waters using a radon-in-air monitor, Environ. Sci. Technol., 35, 4680-4683, 2001.

Kim, G., Hussain, N., and Church, T.: Tracing the advection of organic carbon into the subsurface Sargasso Sea using a $^{228}Ra/^{226}Ra$ tracer, Geophys. Res. Lett., 30, 2003.

Kim, T. -H., Kim, G., Lee, S. A., and Dittmar, T.: Extraordinary slow degradation of Dissolved Organic Carbon (DOC) in a cold marginal sea, Sci. Rep., 5, 13808, doi:10.1038/srep13808, 2015.

Kim, T. -H., Waska, H., Kwon, E., Suryaputra, I. G. N., and Kim, G.: Production,

degradation, and flux of dissolved organic matter in the subterranean estuary of a large tidal flat, Mar. Chem., 142, 1-10, 2012.

Kim, T.-H., Kwon, E., Kim, I., Lee, S.-A., and Kim, G.: Dissolved organic matter in the subterranean estuary of a volcanic island, Jeju: Importance of dissolved organic nitrogen fluxes to the ocean, Journal of sea research, 78, 18-24, 2013.

Kim, T.-W., Kim, D., Baek, S. H., and Kim, Y. O.: Human and riverine impacts on the dynamics of biogeochemical parameters in Kwangyang Bay, South Korea revealed by time-series data and multivariate statistics, Mar. Pollut. Bull., 90, 304-311, 2015b.

Kirkels, F., C. Cerli, E. Federherr, J. Gao, and K. Kalbitz.: A novel high-temperature combustion based system for stable isotope analysis of dissolved organic carbon in aqueous samples. II: optimization and assessment of analytical performance. Rapid Commun. Mass Spectrom. 28: 2574-2586, 2014.

Laane, R.: Conservative behaviour of dissolved organic carbon in the Ems-Dollart estuary and the western Wadden Sea, Neth. J. Sea Res., 14, 192-199, 1980.

Lamb, A. L., Wilson, G. P., and Leng, M. J.: A review of coastal palaeoclimate and relative sea-level reconstructions using δ13C and C/N ratios in organic material. Earth-Sci. Rev, 75(1-4), 29-57, 2006.

Lang, S. Q., Lilley, M. D., and Hedges, J. I.: A method to measure the isotopic (13C) composition of dissolved organic carbon using a high temperature combustion instrument, Mar. Chem., 103, 318-326, 2007.

Lee, C.-W. and Min, B.-Y.: Pollution in Masan Bay, a matter of concern in South Korea, Mar. Pollut. Bull., 21, 226-229, 1990.

Lee, H. J., Hong, S. H., Kim, M., Ha, S. Y., An, S. M., and Shim, W. J.: Tracing origins of sewage and organic matter using dissolved sterols in Masan and

Haengam Bay, Korea, Ocean Sci. J., 46, 95-103, 2011.

Lee, J. S., Kim, K. H., and Moon, D. S. J. J. o. e. r.: Radium isotopes in the Ulsan Bay, 82, 129-141, 2005.

Lee, S.-A., and Kim, G.: Sources, fluxes, and behaviors of fluorescent dissolved organic matter (FDOM) in the Nakdong River Estuary, Korea, Biogeosciences, 15, 1115-1122, 2018.

Lee, Y.-W., Hwang, D.-W., Kim, G., Lee, W.-C., and Oh, H.-T.: Nutrient inputs from submarine groundwater discharge (SGD) in Masan Bay, an embayment surrounded by heavily industrialized cities, Korea, Sci. Total Environ., 407, 3181-3188, 2009.

Liu, C., Du, Y., Yin, H., Fan, C., Chen, K., Zhong, J., and Gu, X.: Exchanges of nitrogen and phosphorus across the sediment-water interface influenced by the external suspended particulate matter and the residual matter after dredging, Environ. Pollut., 246, 207-216, https://doi.org/10.1016/j.envpol.2018.11.092, 2019.

Lobbes, J. M., Fitznar, H. P., and Kattner, G.: Biogeochemical characteristics of dissolved and particulate organic matter in Russian rivers entering the Arctic Ocean, Geochim. Cosmochim. Acta, 64, 2973-2983, 2000.

Lu, Y., J. W. Edmonds, Y. Yamashita, B. Zhou, A. Jaegge, and M. Baxley.: Spatial variation in the origin and reactivity of dissolved organic matter in Oregon-Washington coastal waters. Ocean Dyn. 65: 17-32, 2015

Ludwig, W., Probst, J. L., and Kempe, S.: Predicting the oceanic input of organic carbon by continental erosion, Global Biogeochem. Cycles, 10, 23-41, 1996.

Maher, D. T., I. R. Santos, L. Golsby-Smith, J. Gleeson, and B. D. Eyre.: Groundwater-derived dissolved inorganic and organic carbon exports from a mangrove tidal creek: The missing mangrove carbon sink? Limnol. Oceanogr. 58:

475-488, 2013.

Maie, N., Boyer, J. N., Yang, C., and Jaffé, R.: Spatial, geomorphological, and seasonal variability of CDOM in estuaries of the Florida Coastal Everglades, Hydrobiol., 569, 135-150, 2006.

Mantoura, R. and Woodward, E.: Conservative behaviour of riverine dissolved organic carbon in the Severn Estuary: chemical and geochemical implications, Geochim. Cosmochim. Acta, 47, 1293-1309, 1983.

Markager, S., Stedmon, C. A., and Søndergaard, M.: Seasonal dynamics and conservative mixing of dissolved organic matter in the temperate eutrophic estuary Horsens Fjord, Estuarine Coastal Shelf Sci., 92, 376-388, 2011.

Mayer, L. M., Schick, L. L., and Loder, T. C.: Dissolved protein fluorescence in two Maine estuaries, Mar. Chem., 64, 171-179, 1999.

McCallister, S. L., Bauer, J. E., Ducklow, H. W., and Canuel, E. A.: Sources of estuarine dissolved and particulate organic matter: a multi-tracer approach, Org. Geochem., 37, 454-468, 2006.

McKnight, D. M. and Aiken, G. R.: Sources and age of aquatic humus, in: Aquatic humic substances, Springer, 9-39, 1998.

Meybeck, M.: Carbon, nitrogen, and phosphorus transport by world rivers, Am. J. Sci, 282, 401-450, 1982.

Milliman, J. D., Qinchun, X., and Zuosheng, Y.: Transfer of particulate organic carbon and nitrogen from the Yangtze River to the ocean, Am. J. Sci., 284, 824-834, 1984.

Moore, W. S. and Arnold, R.: Measurement of ^{223}Ra and ^{224}Ra in coastal waters using a delayed coincidence counter, Journal of Geophysical Research: Oceans, 101, 1321-1329, 1996.

Moore, W. S., and D. F. Reid.: Extraction of radium from natural waters using manganese-impregnated acrylic fibers. J. Geophys. Res. 78: 8880-8886, 1973.

Moore, W. S., and Reid, D. F.: Extraction of radium from natural waters using manganese-impregnated acrylic fibers, J. Geophys. Res., 78, 8880-8886, 1973.

Moran, M. A., and Zepp, R. G.: Role of photoreactions in the formation of biologically labile compounds from dissolved organic matter, Limnol. Oceanogr., 42, 1307-1316, 1997.

Moran, M. A., Pomeroy, L. R., Sheppard, E. S., Atkinson, L. P., and Hodson, R. E.: Distribution of terrestrially derived dissolved organic matter on the southeastern US continental shelf, Limnol. Oceanogr., 36, 1134-1149, 1991.

Moran, M. A., Sheldon, W. M., and Zepp, R. G.: Carbon loss and optical property changes during long-term photochemical and biological degradation of estuarine dissolved organic matter, Limnol. Oceanogr., 45, 1254-1264, 2000.

Moyer, R. P., Powell, C. E., Gordon, D. J., Long, J. S., and Bliss, C. M.: Abundance, distribution, and fluxes of dissolved organic carbon (DOC) in four small sub-tropical rivers of the Tampa Bay Estuary (Florida, USA), Appl. Geochem., 63, 550-562, 2015.

Murphy, K. R., Hambly, A., Singh, S., Henderson, R. K., Baker, A., Stuetz, R., Khan, S. J. J. E. S., and Technology: Organic matter fluorescence in municipal water recycling schemes: toward a unified PARAFAC model, 45, 2909-2916, 2011.

Murphy, K. R., Stedmon, C. A., Waite, T. D., and Ruiz, G. M.: Distinguishing between terrestrial and autochthonous organic matter sources in marine environments using fluorescence spectroscopy, Mar. Chem., 108, 40-58, 2008.

Murphy, K. R., Stedmon, C. A., Wenig, P., and Bro, R. J. A. M.: OpenFluor–an online spectral library of auto-fluorescence by organic compounds in the

environment, 6, 658-661, 2014.

Oh, Y. H., Lee, Y.-W., Park, S. R., and Kim, T.-H. J. J. o. M. S.: Importance of dissolved organic carbon flux through submarine groundwater discharge to the coastal ocean: Results from Masan Bay, the southern coast of Korea, 173, 43-48, 2017.

Opsahl, S. P., and Zepp, R. G.: Photochemically-induced alteration of stable carbon isotope ratios ($\delta^{13}C$) in terrigenous dissolved organic carbon, Geophys. Res. Lett., 28, 2417-2420, 2001.

Osburn, C. L., and Stedmon, C. A.: Linking the chemical and optical properties of dissolved organic matter in the Baltic-North Sea transition zone to differentiate three allochthonous inputs, Mar. Chem., 126, 281-294, 10.1016/j.marchem.2011.06.007, 2011.

Osburn, C. L., Wigdahl, C. R., Fritz, S. C., and Saros, J. E.: Dissolved organic matter composition and photoreactivity in prairie lakes of the US Great Plains, Limnol. Oceanogr., 56, 2371-2390, 2011.

Palmer, S. M., D. Hope, M. F. Billett, J. J. Dawson, and C. L. Bryant.: Sources of organic and inorganic carbon in a headwater stream: evidence from carbon isotope studies. Biogeochemistry 52: 321-338, 2001.

Panetta, R. J., Ibrahim, M., and Gélinas, Y.: Coupling a high-temperature catalytic oxidation total organic carbon analyzer to an isotope ratio mass spectrometer to measure natural-abundance $\delta^{13}C$-dissolved organic carbon in marine and freshwater samples, Anal. Chem., 80, 5232-5239, 2008.

Parlanti, E., K. Wörz, L. Geoffroy, and M. Lamotte.: Dissolved organic matter fluorescence spectroscopy as a tool to estimate biological activity in a coastal zone submitted to anthropogenic inputs. Org. Geochem. 31: 1765-1781, 2000.

Peterson, B. J., and B. Fry.: Stable isotopes in ecosystem studies. Annual review of ecology and systematics: 293-320, 1987.

Peterson, B., B. Fry, M. Hullar, S. Saupe, and R. Wright.: The distribution and stable carbon isotopic composition of dissolved organic carbon in estuaries. Estuaries 17: 111-121, 1994.

Pradhan, U., Wu, Y., Shirodkar, P., Zhang, J., and Zhang, G.: Sources and distribution of organic matter in thirty five tropical estuaries along the west coast of India-a preliminary assessment, Estuarine Coastal Shelf Sci., 151, 21-33, 2014.

Qualls, R. G., Haines, B. L., and Swank, W. T.: Fluxes of dissolved organic nutrients and humic substances in a deciduous forest, Ecology, 72, 254-266, 1991.

Raymond, P. A., and Bauer, J. E.: DOC cycling in a temperate estuary: a mass balance approach using natural ^{14}C and ^{13}C isotopes, Limnol. Oceanogr., 46, 655-667, 2001b.

Raymond, P. A., and Bauer, J. E.: Use of ^{14}C and ^{13}C natural abundances for evaluating riverine, estuarine, and coastal DOC and POC sources and cycling: a review and synthesis, Org. Geochem., 32, 469-485, 2001a.

Raymond, P. A., Bauer, J. E., Caraco, N. F., Cole, J. J., Longworth, B., and Petsch, S. T.: Controls on the variability of organic matter and dissolved inorganic carbon ages in northeast US rivers, Mar. Chem., 92, 353-366, 2004.

Raymond, P. A., N.-H. Oh, R. E. Turner, and W. Broussard.: Anthropogenically enhanced fluxes of water and carbon from the Mississippi River. Nature 451: 449, 2008.

Rochelle-Newall, E. J., and T. R. Fisher.: Chromophoric dissolved organic matter and dissolved organic carbon in Chesapeake Bay. Mar. Chem. 77: 23-41, 2002.

Romera-Castillo, C., Sarmento, H., Álvarez-Salgado, X. A., Gasol, J. M., and

Marrasé, C.: Net production and consumption of fluorescent colored dissolved organic matter by natural bacterial assemblages growing on marine phytoplankton exudates, Appl. Environ. Microbiol., 77, 7490-7498, 2011.

Schiff, S., R. Aravena, S. Trumbore, and P. Dillon.: Dissolved organic carbon cycling in forested watersheds: a carbon isotope approach. Water Resour. Res. 26: 2949-2957, 1990.

Schlesinger, W. H., and Melack, J. M.: Transport of organic carbon in the world's rivers, Tellus, 33, 172-187, 1981.

Spiker, E.: The behavior of ^{14}C and ^{13}C in estuarine water: effects of in situ CO2 production and atmospheric exchange, Radiocarbon, 22, 647-654, 1980.

Stedmon, C. A., Markager, S., Søndergaard, M., Vang, T., Laubel, A., Borch, N. H., and Windelin, A.: Dissolved organic matter (DOM) export to a temperate estuary: seasonal variations and implications of land use, Estuaries Coasts, 29, 388-400, 2006.

Steinberg, D. K., Nelson, N. B., Carlson, C. A., and Prusak, A. C.: Production of chromophoric dissolved organic matter (CDOM) in the open ocean by zooplankton and the colonial cyanobacterium Trichodesmium spp, Mar. Ecol. Prog. Ser., 267, 45-56, 2004.

Stepanauskas, R., JØrgensen, N. O., Eigaard, O. R., Žvikas, A., Tranvik, L. J., and Leonardson, L.: Summer inputs of riverine nutrients to the Baltic Sea: bioavailability and eutrophication relevance, Ecological monographs, 72, 579-597, 2002.

Sun, Y., and Torgersen, T.: The effects of water content and Mn-fiber surface conditions on ^{224}Ra measurement by ^{220}Rn emanation, Mar. Chem., 62, 299-306, 1998.

Thornton, S., and McManus, J.: Application of organic carbon and nitrogen stable isotope and C/N ratios as source indicators of organic matter provenance in estuarine systems: evidence from the Tay Estuary, Scotland, Estuarine Coastal Shelf Sci., 38, 219-233, 1994.

Tremblay, L., and Benner, R.: Microbial contributions to N-immobilization and organic matter preservation in decaying plant detritus, Geochim. Cosmochim. Acta, 70, 133-146, 2006.

Twardowski, M. S. and Donaghay, P. L.: Separating in situ and terrigenous sources of absorption by dissolved materials in coastal waters, Journal of Geophysical Research: Oceans (1978–2012), 106, 2545-2560, 2001.

Vignudelli, S., Santinelli, C., Murru, E., Nannicini, L., and Seritti, A.: Distributions of dissolved organic carbon (DOC) and chromophoric dissolved organic matter (CDOM) in coastal waters of the northern Tyrrhenian Sea (Italy), Estuarine Coastal Shelf Sci., 60, 133-149, 2004.

Wang, X.-C., Chen, R. F., and Gardner, G. B.: Sources and transport of dissolved and particulate organic carbon in the Mississippi River estuary and adjacent coastal waters of the northern Gulf of Mexico, Mar. Chem., 89, 241-256, 2004.

Willey, J. D., R. J. Kieber, M. S. Eyman, and G. B. Avery.: Rainwater dissolved organic carbon: concentrations and global flux. Global Biogeochem. Cycles 14: 139-148, 2000.

Wünsch, U. J., Murphy, K. R., Stedmon, C. A. J. E. s., and technology: The one-sample PARAFAC approach reveals molecular size distributions of fluorescent components in dissolved organic matter, 51, 11900-11908, 2017.

Ya, C., Anderson, W., and Jaffé, R.: Assessing dissolved organic matter dynamics and source strengths in a subtropical estuary: Application of stable carbon isotopes

and optical properties, Cont. Shelf Res., 92, 98-107, 2015.

Yoo, K.: Population dynamics of dinoflagellate community in Masan Bay with a note on the impact of environmental parameters, Mar. Pollut. Bull., 23, 185-188, 1991.

Zepp, R. G., Sheldon, W. M., and Moran, M. A.: Dissolved organic fluorophores in southeastern US coastal waters: correction method for eliminating Rayleigh and Raman scattering peaks in excitation–emission matrices, Mar. Chem., 89, 15-36, 2004.

Zhang, Y., van Dijk, M. A., Liu, M., Zhu, G., and Qin, B.: The contribution of phytoplankton degradation to chromophoric dissolved organic matter (CDOM) in eutrophic shallow lakes: field and experimental evidence, Water Res., 43, 4685-4697, 2009.

Zhao, Z., Gonsior, M., Luek, J., Timko, S., Ianiri, H., Hertkorn, N., Schmitt-Kopplin, P., Fang, X., Zeng, Q., and Jiao, N.: Picocyanobacteria and deep-ocean fluorescent dissolved organic matter share similar optical properties, Nat. Commun., 8, 2017.

Abstract (Korean)

연안 용존유기물(DOM)은 해양 생태계와 탄소와 영양염의 생지화학적 순환에 중요한 역할을 한다. DOM의 거동과 순환은 DOM의 기원과 조성에 매우 큰 영향을 받는다. 해양환경에서 DOM의 기원과 플럭스를 연구하는 것은 매우 중요함에도 불구하고 연안 환경의 복잡성 때문에 여전히 잘 알려져 있지 않다. 따라서 본 연구에서는 용존유기탄소(DOC), 용존유기질소(DON), 안정탄소동위원소(δ^{13}C-DOC), 유색용존유기물(FDOM)과 같은 다양한 DOM 성분을 측정하여 서로 다른 연안 환경에서 DOM의 기원과 플럭스를 알아보고자 하였다.

이를 위해, 고도의 산업화된 도시인 마산만에서 2011년 8월과 2016년 8월 2회에 걸쳐 시료를 채취하였다. 2011년 시료의 경우, 높은 염분대(16-21)에서 과잉 DOC농도가 관찰되었고 이는 -23.7‰에서 -20.6‰의 δ^{13}C-DOC 값과 높은 농도의 단백질 기원 FDOM, 낮은 DOC/DON 비 값(8-15)을 고려해볼 때 해양의 생물생산에 의한 기원으로 판단된다. 반면, 2016년의 고염분에서 나타난 높은 DOC 농도는 낮은 FDOM 농도, -28.8‰에서 -21.1‰의 낮은 δ^{13}C-DOC, 높은 C/N 비 값(13-45)의 특징으로 보아 육상과 해양의 상호작용으로 인한 육상 C3 식물 기원으로 판단된다. 본 연구결과에서 δ^{13}C-DOC, FDOM, C/N 비 값 등과 같은 다양한 추적자를 함께 사용하는 것은 연안 DOM의 복잡한 기원을 밝혀내는데 강력한 도구임을 보여주었다.

두번째 연구에서는 한국에서 가장 긴 강의 하구에 위치한 낙동강 하구역에서 시료를 채취하였다. 하구의 시료는 댐의 하류에 위치한 고정된 장소에서 2014년 10월부터 2015년 8월까지 매월 사리시에 매 시간마다 24시간동안 채취하였다. DOC와 휴믹물질 FDOM는 염분에 대해 강한 음의 상관관계를 보였고, 이는 강에서 유입된 DOM이 주요 기원이며 하구에서 보존적으로 혼합됨을 시사한다. δ^{13}C−DOC(−27.5‰에서 − 24.5‰) 값은 이 두 성분이 육상기원이라는 것을 뒷받침해준다. 휴믹물질 FDOM의 염분에 대한 기울기는 휴믹물질이 활발하게 생성되는 여름과 가을에 60−80% 더 높게 나타났다. 단백질기원 FDOM의 염분에 대한 기울기는 강에서의 높은 생물생산에 의해 봄철에 70−80% 더 높게 나타났다. 이러한 결과는 해양으로 유출되는 휴믹과 단백질 FDOM의 강유출량이 계절에 따라 큰 차이를 보인다는 것을 시사한다.

연안에서 DOM과 영양염의 기원, 생물학적 변형, 플럭스를 알아보기 위해 한국의 세 만 (광양만, 수영만, 울산만)에서 해수 시료를 채취하였다. 또한 만의 체류시간과 플럭스를 산정하기 위해 라듐 동위원소 (^{223}Ra, ^{224}Ra, and ^{226}Ra)를 측정하였다. 라듐 비 값을 이용하여 계산한 광양만, 수영만, 울산만의 체류시간은 각각 15일, 1.9일, 1.5일로 산정되었다. 울산만은 짧은 체류시간으로 인해 DOC, DIN, DIP은 육상과 해양의 두 단성분의 혼합형태가 나타났다. 수영만의 DOC, DIN, DIP은 해양과 육상 단성분의 보존적 혼합분포와 높은 염분대에서 과잉의 DOC 농

도분포인 두 분포가 나타났다. 체류시간이 가장 긴 광양만은 DIN과 DIP가 완전히 고갈되었으며 DOC와 DON는 증가된 농도가 나타났다. 수영만의 과잉 DOC는 δ^{13}C−DOC 값을 고려하여 볼 때 해양 생성 기원으로 판단된다. 육상기원 휴믹 FDOM은 세 만 전체에서 보존적인 혼합이 나타났다. 라듐 동위원소를 이용하여 계산한 체류시간으로 산정한 플럭스에서 광양만은 DOC와 DON의 소스, DIN과 DIP의 제거 기작이 활발하며 수영만과 울산만은 무기 영양염의 공급이 활발한 것으로 나타났다. 따라서 이 연구에서는 연안 만지역에서 체류시간이 DOM과 영양염의 생지화학적 생성과 변형에 중요한 역할을 한다는 것을 알아내었다. 또한 δ^{13}C−DOC, FDOM, C/N비값과 같은 다양한 DOM 추적자와 Ra 동위원소를 함께 사용하는 것은 연안해역에서 복잡한 DOM과 영양염의 기원과 플럭스를 알아내는데 좋은 추적자로 사용될 수 있음을 시사한다.

주요어: 용존유기탄소; 형광용존유기물질; 용존유기질소; 안정탄소동위원소; 라듐 동위원소; 연안해역

학번: 2010−23135

Appendix: Supporting materials

Table S1. The concentrations of $FDOM_H$, $FDOM_P$, and DOC, and the values of $\delta^{13}C$ in DOC in the Nakdong-River Estuary.

Oct. 23 2014	time	Salinity	$FDOM_H$ (QSU)	$FDOM_P$ (QSU)	DOC (μM)	$DO^{13}C$ (‰)
1	15:00	0.23	16.3	15.8	229	-25.4
2	16:00	0.33	13.9	13.6	220	-
3	17:00	0.40	14.7	14.2	219	-23.8
4	18:00	0.18	15.6	16.2	232	-
5	19:00	0.17	14.1	15.2	n/a	-
6	20:00	0.31	14.2	14.7	230	-24.6
7	21:00	0.20	16.0	15.9	218	-24.9
8	22:00	0.59	14.2	14.4	225	-
9	23:00	4.51	12.5	13.3	203	-25.0
10	0:00	2.54	14.5	15.1	213	-
11	1:00	3.17	13.0	13.2	n/a	-25.7
12	2:00	3.72	13.1	12.9	207	-
13	3:00	3.27	12.2	12.2	191	-25.4
14	4:00	2.46	14.4	14.5	199	-
15	5:00	2.42	14.8	14.6	207	-25.6
16	6:00	2.88	14.8	14.1	194	-
17	7:00	3.61	13.8	13.5	193	-25.5
18	8:00	8.40	11.4	12.0	171	-
19	9:00	9.85	7.6	7.6	152	-24.3
20	10:00	17.88	11.6	11.7	180	-
21	11:00	14.15	8.3	8.7	146	-23.7
22	12:00	11.82	10.3	11.4	168	-
23	13:00	5.36	12.3	14.3	206	-25.5
24	14:00	3.11	13.1	16.9	212	-
Nov. 24 2014						
1	14:00	19.22	6.4	5.8	145	-24.2
2	15:00	18.71	6.4	6.3	153	-
3	16:00	16.99	7.1	7.1	160	-24.7
4	17:00	16.83	7.0	6.7	156	-

5	18:00	16.86	7.0	6.7	153	-24.3
6	19:00	18.10	6.6	6.0	150	-
7	20:00	17.00	6.9	6.3	153	-24.0
8	21:00	18.08	6.9	6.4	158	-
9	22:00	19.98	5.6	5.5	138	-23.9
10	23:00	22.25	5.0	5.0	129	-
11	0:00	17.92	6.3	5.9	144	-25.1
12	1:00	15.69	7.1	6.5	156	-
13	2:00	16.11	7.1	8.0	149	-25.2
14	3:00	14.15	7.7	6.9	156	-
15	4:00	12.38	8.8	7.9	162	-24.5
16	5:00	10.56	9.2	8.1	168	-
17	6:00	10.44	8.9	8.1	167	-23.1
18	7:00	8.66	9.4	8.8	173	-
19	8:00	10.18	9.0	8.1	166	-23.5
20	9:00	12.42	8.4	7.6	160	-
21	10:00	16.27	6.8	6.4	141	-25.4
22	11:00	17.96	6.6	6.3	144	-
23	12:00	25.37	4.3	4.9	110	-21.1
24	13:00	20.01	5.8	5.6	132	-
Dec. 22 2014						
1	14:00	21.31	5.2	11.9	n/a	-
2	15:00	20.26	5.6	9.5	154	-22.1
3	16:00	19.72	5.4	9.6	159	-
4	17:00	17.59	6.0	10.5	163	-22.2
5	18:00	17.65	5.7	10.2	149	-
6	19:00	17.09	6.3	11.3	162	-22.2
7	20:00	18.45	5.6	9.9	150	-
8	21:00	18.90	5.6	9.4	150	-22.7
9	22:00	20.48	4.8	8.5	148	-
10	23:00	21.83	4.6	8.0	144	-21.5
11	0:00	22.87	4.5	7.4	135	-
12	1:00	22.14	4.5	7.6	128	-21.5
13	2:00	23.02	3.9	6.5	123	-
14	3:00	23.75	4.0	6.3	117	-21.0
15	4:00	24.33	3.7	5.8	110	-
16	5:00	25.86	3.3	5.0	105	-20.4

17	6:00	24.55	3.8	6.0	111	-
18	7:00	24.97	4.0	5.5	106	-17.6
19	8:00	25.09	3.6	5.6	127	-
20	9:00	25.11	3.7	5.8	107	-20.2
21	10:00	24.38	3.6	5.9	106	-
22	11:00	25.85	3.2	4.9	103	-19.8
23	12:00	23.20	3.7	5.6	104	-
24	13:00	23.46	4.1	6.8	107	-21.4
Jan. 21 2015						
1	14:00	27.08	2.8	6.8	n/a	-
2	15:00	25.65	3.0	5.4	118	-22.2
3	16:00	23.15	3.5	5.5	125	-
4	17:00	17.48	5.0	7.4	145	-22.9
5	18:00	16.92	5.2	7.5	144	-
6	19:00	15.61	5.6	7.8	149	-24.6
7	20:00	16.12	5.4	7.3	142	-
8	21:00	18.32	5.0	6.9	131	-
9	22:00	18.28	5.1	7.3	140	-
10	23:00	19.50	5.0	7.1	134	-22.2
11	0:00	21.74	3.7	6.3	133	-
12	1:00	24.84	3.1	4.8	110	-20.1
13	2:00	26.88	2.6	4.5	107	-
14	3:00	25.73	2.9	5.3	109	-19.6
15	4:00	24.31	3.2	5.2	116	-
16	5:00	23.33	3.6	5.4	113	-21.5
17	6:00	19.95	4.4	6.4	128	-
18	7:00	19.41	4.6	6.5	128	-23.0
19	8:00	23.88	3.2	4.6	112	-
20	9:00	25.93	0.1	0.7	104	-20.5
21	10:00	23.08	3.3	4.9	115	-22.4
22	11:00	23.51	3.3	5.5	105	-19.8
23	12:00	23.97	3.1	4.6	117	-21.2
24	13:00	24.55	3.3	4.9	120	-21.4
Feb. 23 2015						
1	12:00	20.59	4.5	8.4	n/a	-
2	13:00	23.30	4.0	7.8	121	-22.2

3	14:00	25.98	3.6	6.7	113	-
4	15:00	25.36	3.6	6.6	119	-22.9
5	16:00	23.05	3.9	7.6	119	-
6	17:00	19.12	5.0	9.5	132	-24.6
7	18:00	18.13	5.0	9.5	136	-
8	19:00	18.44	5.1	9.3	130	-
9	20:00	19.33	4.6	8.6	123	-
10	21:00	19.83	5.0	8.9	123	-22.2
11	22:00	17.01	4.9	9.2	125	-
12	23:00	17.46	4.9	9.1	126	-20.1
13	0:00	20.92	4.5	7.8	110	-
14	1:00	22.69	3.8	6.6	107	-19.6
15	2:00	24.41	3.6	6.1	103	-
16	3:00	25.83	3.1	5.3	102	-21.5
17	4:00	24.21	3.4	6.1	106	-
18	5:00	24.27	3.4	5.9	104	-23.0
19	6:00	22.38	3.9	6.8	111	-
20	7:00	24.61	3.3	5.9	103	-20.5
21	8:00	25.78	3.0	5.1	99	-
22	9:00	24.16	3.5	6.3	108	-
23	10:00	24.03	3.5	6.3	108	-
24	11:00	22.27	3.9	7.2	109	-
Mar. 22 2015						
1	11:00	16.12	4.8	22.4	n/a	-23.2
2	12:00	19.12	4.3	12.0	141	-
3	13:00	11.29	5.5	15.8	161	-22.5
4	14:00	10.96	6.0	16.4	161	-
5	15:00	5.43	7.1	19.4	183	-23.4
6	16:00	4.83	7.1	20.1	174	-
7	17:00	3.35	7.4	20.9	177	-23.8
8	18:00	3.98	7.2	20.2	185	-
9	19:00	3.46	7.3	20.3	186	-24.4
10	20:00	7.50	6.5	17.5	166	-
11	21:00	8.86	6.1	16.2	164	-23.9
12	22:00	11.72	5.5	15.0	148	-
13	23:00	14.44	5.7	14.8	142	-23.3
14	0:00	14.06	5.4	14.1	143	-

15	1:00	17.15	4.7	11.4	127	-23.4
16	2:00	17.23	5.8	12.3	132	-
17	3:00	17.08	4.8	11.7	134	-22.8
18	4:00	14.81	5.3	13.9	134	-
19	5:00	15.17	6.1	12.4	137	-23.8
20	6:00	15.65	5.4	12.7	137	-
21	7:00	16.64	4.7	11.8	142	-23.2
22	8:00	15.76	9.1	11.5	135	-
23	9:00	15.96	5.1	12.3	137	-23.7
24	10:00	17.75	4.6	11.1	126	-
Apr. 21 2015						
1	10:00	3.23	9.8	15.8	n/a	-25.7
2	11:00	5.32	9.0	13.0	174	-
3	12:00	8.88	7.6	10.6	152	-25.0
4	13:00	10.14	7.3	10.7	147	-
5	14:00	5.76	8.1	11.6	160	-24.7
6	15:00	4.45	8.5	12.1	163	-
7	16:00	2.46	9.1	12.8	172	-25.7
8	17:00	1.79	9.1	12.6	169	-
9	18:00	1.39	8.4	13.1	170	-25.6
10	19:00	0.78	8.2	12.1	164	-
11	20:00	1.86	7.9	13.2	165	-25.4
12	21:00	1.71	8.2	11.9	163	-
13	22:00	2.88	7.6	11.6	160	-26.5
14	23:00	5.56	7.4	10.1	148	-
15	0:00	12.18	5.9	8.2	133	-23.3
16	1:00	11.03	6.3	8.6	145	-
17	2:00	9.23	6.6	8.7	155	-24.8
18	3:00	7.94	7.1	9.4	160	-
19	4:00	6.66	7.7	10.9	163	-25.6
20	5:00	5.92	9.1	11.7	171	-
21	6:00	5.00	8.9	12.4	163	-24.9
22	7:00	3.28	9.2	14.2	172	-
23	8:00	3.03	9.1	12.4	171	-25.3
24	9:00	3.33	9.2	12.3	172	-
May 19 2015						

1	17:00	13.90	6.3	7.1	n/a	-
2	18:00	13.76	6.8	6.1	156	-
3	19:00	13.32	6.9	6.1	147	-
4	20:00	16.06	6.2	4.8	143	-24.6
5	21:00	15.45	6.1	6.3	146	-
6	22:00	16.03	6.0	6.8	145	-21.8
7	23:00	16.83	5.6	6.6	139	-
8	0:00	19.33	5.1	4.8	133	-21.8
9	1:00	15.75	5.7	5.1	135	-
10	2:00	14.97	6.2	5.3	142	-23.2
11	3:00	15.18	5.9	5.1	143	-24.6
12	4:00	n/a	n/a	n/a	n/a	-
13	5:00	13.10	6.3	5.3	148	-
14	6:00	12.21	6.6	5.5	154	-23.9
15	7:00	11.48	7.0	5.8	152	-
16	8:00	13.87	6.9	5.7	163	-24.4
17	9:00	11.19	6.2	5.2	155	-
18	10:00	16.49	6.5	5.6	148	-23.5
19	11:00	20.08	5.3	5.3	132	-
20	12:00	23.75	4.4	5.9	123	-22.2
21	13:00	22.43	0.4	0.6	126	-
22	14:00	22.66	2.5	3.2	137	-22.6
23	15:00	n/a	n/a	n/a	n/a	-
24	16:00	19.22	5.9	6.1	162	-24.0
Jun. 18 2015						
1	14:00	23.96	4.3	5.8	147	
2	15:00	22.58	4.4	5.1	142	-24.9
3	16:00	21.85	4.6	4.8	135	
4	17:00	22.53	4.4	4.8	137	-22.7
5	18:00	24.57	3.8	4.0	128	
6	19:00	25.93	3.5	3.6	120	-21.8
7	20:00	26.30	3.4	3.4	113	
8	21:00	26.45	3.3	3.6	113	-20.6
9	22:00	26.78	3.1	3.3	111	
10	23:00	26.78	3.1	3.4		-20.7
11	0:00	28.49	2.8	3.7	112	
12	1:00	28.46	2.9	3.7	109	-20.0

13	2:00	27.46	3.1	3.6	118	
14	3:00	26.39	3.2	3.6	121	-21.3
15	4:00	26.05	3.3	3.4	128	
16	5:00	25.13	3.7	3.9	130	-21.3
17	6:00	25.26	3.3	3.3	126	
18	7:00	26.87	3.0	3.1	119	-20.7
19	8:00	26.72	3.0	3.2	118	
20	9:00	26.40	2.9	3.1	120	-19.2
21	10:00	27.17	2.6	3.0	114	
22	11:00	28.31	2.4	3.0	115	-18.8
23	12:00	25.28	3.2	4.0	124	
24	13:00	25.19	3.3	4.2	129	-21.6
Jul. 15 2015						
1	11:00	8.33	16.4	8.7	250	-24.8
2	12:00	6.02	17.3	7.5	245	-25.2
3	13:00	2.37	19.7	7.5	249	-25.5
4	14:00	2.38	19.2	7.6	256	-25.7
5	15:00	1.82	19.4	7.3	257	-25.5
6	16:00	2.15	19.3	7.3	253	-25.3
7	17:00	2.55	19.1	7.4	256	-25.9
8	18:00	3.31	18.9	6.9	250	-25.2
9	19:00	3.76	18.9	6.7	244	-25.1
10	20:00	5.42	17.9	6.0	237	-24.8
11	21:00	7.74	16.9	5.7	226	-24.7
12	22:00	15.23	11.6	5.0	187	-23.9
13	23:00	14.28	11.9	4.3	190	-23.9
14	0:00	8.29	15.2	5.0	222	-24.9
15	1:00	5.37	17.3	5.0	231	-25.4
16	2:00	3.89	18.2	5.1	249	-25.5
17	3:00	3.37	17.9	5.3	242	-25.6
18	4:00	3.39	18.6	7.1	262	-25.5
19	5:00	3.39	18.2	6.9	256	-24.9
20	6:00	n/a	n/a	n/a	n/a	-
21	7:00	3.49	19.0	6.3	253	-25.1
22	8:00	3.45	19.1	7.7	291	
23	9:00	n/a	n/a	n/a	n/a	-
24	10:00	n/a	n/a	n/a	n/a	-

Aug. 26 2015						
1	12:00	2.91	13.5	7.8	245	-28.2
2	13:00	2.58	13.4	8.1	220	-
3	14:00	2.74	13.7	7.5	212	-26.3
4	15:00	3.17	13.4	7.3	209	-
5	16:00	4.13	13.1	7.2	206	-25.9
6	17:00	4.36	12.1	6.5	199	-
7	18:00	4.71	12.4	6.7	194	-26.2
8	19:00	5.07	12.0	6.4	195	-
9	20:00	6.22	12.1	6.5	189	-24.9
10	21:00	10.99	10.9	6.4	183	-
11	22:00	9.42	11.0	6.0	186	-25.6
12	23:00	6.67	11.3	5.9	194	-
13	0:00	7.69	13.1	6.9	190	-26.9
14	1:00	5.15	13.4	6.8	192	-
15	2:00	4.16	14.3	7.5	194	-26.1
16	3:00	3.85	14.8	7.3	194	-
17	4:00	4.44	13.0	6.8	191	-25.6
18	5:00	5.61	12.5	6.6	187	-
19	6:00	6.34	12.0	6.3	190	-26.3
20	7:00	8.84	11.3	6.0	182	-
21	8:00	10.01	11.2	6.6	182	-27.8
22	9:00	10.68	11.2	6.0	175	-
23	10:00	11.12	11.1	6.6	174	-25.2
24	11:00	n/a	n/a	n/a	n/a	-